Electronic Supplementary Material (ESI) for Journal of Materials Chemistry B.

High nuclearity carbonyl clusters as near-IR contrast agents for photoacoustic in vivo imaging

Zhiyong Lam,‡[ab] Ghayathri Balasundaram,‡[b] Kien Voon Kong,[c] Bo Yang Chor,[a] Douglas Goh,[b] Bahareh Khezri,[a] Richard D. Webster,[a] Weng Kee Leong*[a] and Malini Olivo*[bd]

[a] Division of Chemistry and Biological Chemistry, Nanyang Technological University, Singapore
[b] Singapore Bioimaging Consortium, Agency for Science and Technology and Research (A*STAR), Singapore
[c] Department of Chemistry, National Taiwan University, Taiwan
[d] School of Physics, National University of Ireland, Galway, Ireland
‡ These authors contributed equally

List of contents

1. Experimental section

a. General methods

All reactions and manipulations were carried out under an argon atmosphere using standard Schlenk techniques. Solvents that were used for reaction were distilled over the appropriate drying agents under argon before use. Purification of compounds was generally carried out by column chromatography on silica gel, or by preparative thin-layer chromatography (TLC) using 20 cm x 20 cm plates pre-coated with silica gel 60 F_{254} Infrared (IR) spectra were recorded on a Bruker Alpha FT-IR spectrometer. Solution spectra were recorded in DCM solution, unless otherwise stated, in a solution IR cell with NaCl windows and a path length of 0.1 mm, at a resolution of 2 cm^{-1}. Alternatively, IR spectra of aqueous samples were recorded by drop casting the mixture (10 μL) onto a CaF_2 disc, followed by drying under a stream of nitrogen before recording on the spectrometer. Optical absorption spectra were recorded using a Hitachi U-2900 double-beam spectrophotometer using quartz cuvette with path length of 10 mm. For samples of smaller volume (100 μL), the optical absorption spectra were recorded using a Beckman Coulter DU 730 spectrometer. HRMS were recorded in ESI mode on a Waters UPLC-Q-Tof MS mass spectrometer.

Compounds **1**-**8** were synthesized according to reported methods with slight modifications.[1-7] $Os_3(CO)_{12}$ and $Ru_3(CO)_{12}$ were purchased from Oxkem Ltd. $[(Ph_3P)_2N]Cl$ and indocyanine green (ICG) were purchased from Sigma Aldrich. All other chemical reagents were purchased from other commercial sources and used without further purification.

b. Synthesis of cluster 9

The synthesis was adapted from the microwave-assisted synthesis of cluster **8**.[7] A Discover-SP microwave reactor (2450 MHz, CEM Corp., Matthews, NC) and thick-walled 35 mL glass vessel with Teflon-lined caps (CEM Corp., Matthews, NC) were used. In a typical reaction, a 35 mL microwave vessel was charged with $Os_3(CO)_{12}$ (150 mg, 0.1654 mmol) and diglyme (7 mL). The mixture was irradiated with 300 W with high stirring rate, till the temperature reached 230 ^oC. The power was subsequently reduced to 100 W for additional heating for 10 min. The reaction mixture was cooled to 50 ^oC and vented, before irradiated at 300 W for 4 min. The cooling, venting and irradiation at 300 W for 4 min was repeated once. The solvent was removed by evaporation over a hot water bath and the residue was extracted with acetone (20 mL) and

filtered over a thin layer of celite. The solvent was removed and the residue dissolved in MeOH (10 mL). NaCl (20 mg, 0.34 mmol) was added to the solution and stirred at 60 ^{o}C for 1 h. Solvent was removed and the residue was purified by TLC using acetone-hexane (3:2, v/v) as eluant to give cluster **9** as a dark red band.

Yield: 33 mg (24 %)

R_f = 0.23

IR (acetonitrile, cm^{-1}): ν_{CO} 2038s, 1990s.

HRMS-ESI: *m*/*z* 1294.0946 $[M]^{2-}$ (see figure S26 for isotopic pattern)

c. Cell culture and cell viability assay

Experimental cultures of oral squamous cell carcinoma (OSCC) cell line were obtained from the American Type Culture Collection (ATCC) and cultured in tissue culture dishes (Nunc Inc., IL). The cells were maintained in Dulbecco's modified Eagle's medium (DMEM; Biowest, France) supplemented with 10 % fetal bovine serum (FBS; Gibco®, NY), 1 % L-glutamine (PAA Laboratories, Austria), and 1 % penicillin/streptomycin (HyClone, UT) at 37 °C in 5 % CO_2 atmosphere. Phosphate-buffered saline (PBS) was obtained from PAA Laboratories. Stock solutions of cluster **9** and $[(Ph_3P)_2N]Cl$ in sterile-filtered dimethyl sulfoxide (DMSO) were prepared and serial diluted to lower concentrations. For treatment with the compounds, cells were seeded in wells within 96-well plate in growth medium at the same initial density of 10 000 cells per well, and allowed to adhere and grow for 24 h. They were serum-starved in serum-free DMEM for 24 h, followed by treatment with the indicated concentrations of compounds in serum-free DMEM (1 % DMSO) for 24 h. Control cells were treated with vehicle (1 % DMSO). To each well, 10 µL of MTS reagent (MTS Cell Proliferation Assay Kit, BioVision, CA) was added and then left to incubate in a 37 °C incubator with 5% CO_2 for 2 h. The absorbance intensities at 490 nm were then measured and the cell proliferation relative to the control sample was calculated. Each sample was analyzed in triplicates and was corrected with background intensities from same incubation conditions without the cells. IC_{50} was determined from three separate experiments and the mean value calculated.

d. Gel electrophoresis

Agarose gel (1%, UltraPure™ Agarose, Invitrogen) was cast with and immersed in 0.5 x TAE (Tris-acetate-EDTA buffer, prepared from 50 x stock solution, pH 8.0, 1st BASE). Cluster **9** incubated in 10% DMSO in modified DMEM (30 μL) for different duration (10 min, 1, 3, 5 and 7 days) was loaded into the respective wells of the gel and electrophoresed in a horizontal electrophoresis system (Wide Mini-sub® cell GT Basic System, Biorad, electrode spacing of 15 cm) at 150 V for 30 min.

e. Multispectral optoacoustic tomography (MSOT) experimental parameters and protocol

All phantom and *in vivo* mouse imaging experiments were performed using a real-time MSOT imaging system; inVision 128 (ithera Medical GmbH, Germany).[8] Optical excitation was provided by an optical parametric oscillator with a tunable NIR wavelength range from 680 to 900 nm, which was in turn pumped by a Q-switched Nd:YAG laser with a pulse duration of 10 ns and repetition rate of 10 Hz. Light was delivered by a fiber bundle divided into 10 output arms to illuminate the sample from multiple angles around the imaging plane. PA signals were acquired using a 128-element concave transducer array spanning a circular arc of 270°. This transducer array had a central frequency of 5 MHz, which provided a transverse spatial resolution in the range of 150–200 μm. One transverse image slice was acquired from each laser pulse, resulting in a frame rate of 10 Hz. During image acquisition, the sample was translated through the transducer array along its axis across the volume region of interest (ROI), in order to capture the corresponding transverse image slices.

f. Evaluation of PA activity of clusters 4-9 in phantom model

The phantom is made of polyurethane and is cylindrical in shape with a diameter of 2 cm, which is specially designed to mimic the shape, size, and optical properties of the mouse. In addition, it has two inner cylindrical channels, each with an inner diameter of 3 mm, one for holding the control medium and the other for holding the dissolved contrast agent in the same medium. The control medium and contrast agent suspension (170 μL each) were pipetted into the respective channels of the phantom, and placed in the MSOT imaging chamber using a phantom holder. For data acquisition, we set up an ROI of multiple transverse slices with a step size of 1

mm across the channel portion which contained the probe and control, applied excitation wavelengths from 680 to 900 nm with an interval of 10 nm for each transverse slice, and recorded the averaged PA signals from 10 frames for each wavelength and position. The acquired images were reconstructed using model based approach and PA signals were quantified using ViewMSOT at the respective λ_{max} of each probe from the reconstructed images.[9] The PA amplitude of the probe was determined by subtracting the values of the channel containing the control from that of the probe, and the mean was calculated from 10 different transverse slices.

g. *In vivo* longitudinal monitoring of probe biodistribution in mouse xenograft model

All animal experiments were performed in compliance with the protocol #120774 and #151085 approved by the Institutional Animal Care and Use Committee, Agency for Science, Technology and Research (A*STAR). Xenograft models were established on three Balb/C nude mice by injecting subcutaneously into the right flank of each mouse, a cell suspension (0.1 mL) containing 5×10^6 oral squamous carcinoma cells (OSCC) and matrigel (BD Biosciences, San Jose, CA) in a 1:1 volume ratio. When the tumor volume reached a palpable size, a solution of **9** (200 μL, 500 μM) in 10% DMSO in heparinized saline (v/v) was injected intravenously through the tail vein of each mouse anaesthetized under isoflurane. Ultrasound gel was applied on the mouse skin surface for *in vivo* imaging, and measurements were recorded in temperature-controlled water medium for good acoustic coupling. An animal holder with a thin polyethylene membrane was used to prevent direct contact between the mouse and the water. Seven laser excitation wavelengths (680, 700, 730, 750, 810, 850, and 900 nm) were chosen for multispectral imaging on the basis of the absorption maxima and minima of the contrast agent, and oxy- and deoxyhemoglobin. PA signals were acquired across multiple transverse slices from the liver to the lower abdomen region inclusive of the tumor at a step size of 0.5 mm and averaged over 10 frames for each wavelength.

h. Image processing and analysis for *in vivo* experiments

Images acquired from the *in vivo* experiments were reconstructed using direct back projection approach for offline analysis. After image reconstruction, spectral unmixing was performed to resolve individual components from different chromophores in the system. For each pixel, the

method fits the total measured optoacoustic spectrum to the known absorption spectra of the individual chromophores, based on least-squares linear regression. Images were exported out from ViewMSOT and further analyzed using Fiji (version 2.0.0), an open source image-processing package.[10] Regions of Interest (ROIs) were chosen from liver, spleen, kidney and tumor and quantified for multispectrally unmixed PA signals before and after probe injection. PA signals at all time-points were normalized against that of the pre-injection scan and expressed as fold change over the same.

i. Microwave acid digestion and ICP-MS analysis of osmium content of tissue samples

The mice were euthanized after 24 and 96 h respectively, the organs extracted, washed with deionized water and snap-freezed in liquid nitrogen for future use. The selected organs were freeze-dried over a period of five days and the dried masses measured, prior to microwave acid digestion. A programmable Milestone microwave system (ETHOS EZ, Italy) was used to digest and prepare the samples for ICP analysis. Samples were placed inside the Teflon microwave vessels and 12 mL HCl (37%, ultrapure grade, J. T. Baker, Canada) were added. Ultra-pure water with 18.2 MΩ•cm resistivity was used (ELGA, PURLAB Option – Q, UK) for sample and standard preparations. Using the microwave radiation (Power 1100W) the temperature was ramped to 185 °C in 20 min and then held at that temperature for 15 min. The vessels were opened after cooling down to room temperature for several hours, to prevent any sample loss. The extracts were diluted with ultrapure water, filtered through 0.2 µm syringe filters, and carefully transferred to ICP sample vials for elemental analysis. Samples were analyzed using an Agilent 7700 series ICP-MS (Japan) equipped with a third generation He reaction / collision cell (ORS3) to minimize interference. An external calibration curve for osmium was constructed, before each analytical run, from serial dilutions of an osmium standard for ICP-MS (1000 mgL^{-1}, Inorganic Venture, Christiansburg, VA, USA) with high purity deionized water.

j. Histopathology of organ tissues of mice

Six mice were intravenously injected with cluster **9** (200 μL, 500 μM, 10% DMSO in saline) and euthanized after 24 h and 96 h (three mice at each time point) respectively. For the control sample, four mice were injected with 10% DMSO in saline instead. The mice were anaesthetized using ketamine (150 mg/mL) and xylazine (10 mg/kg) and euthanized by cervical dislocation to collect various organs for histopathology analysis. All organs were immediately fixed in 10% neutral buffered formalin (Sigma) and submitted to the Advanced Molecular Pathology Laboratory (AMPL), IMCB for histopathology evaluation. The pathology report was prepared by an experienced pathologist. All bright field images were captured using the Nikon Ni-E upright microscope, with Plan Apo 20x DIC M N2 objective and Nikon DS-Ri2 camera. The images were viewed using NIS-Elements software.

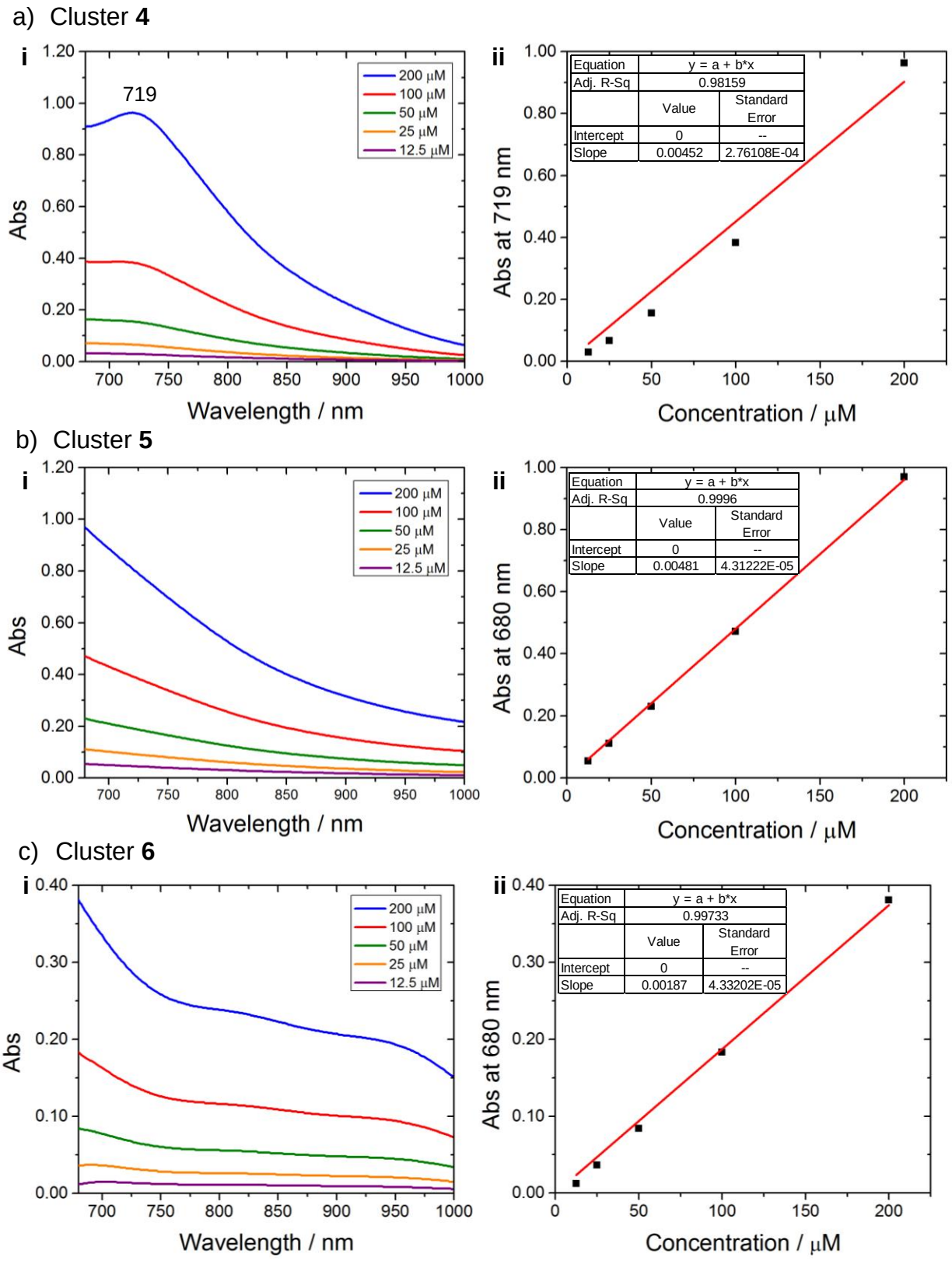

Figure S1. i) Optical absorption spectra of various concentrations (in DMSO), ii) plot of optical absorbance (at respective λ_{max}) as a function of concentrations of a) cluster **4**, b) cluster **5** and cluster **6**.

d) Cluster **7**

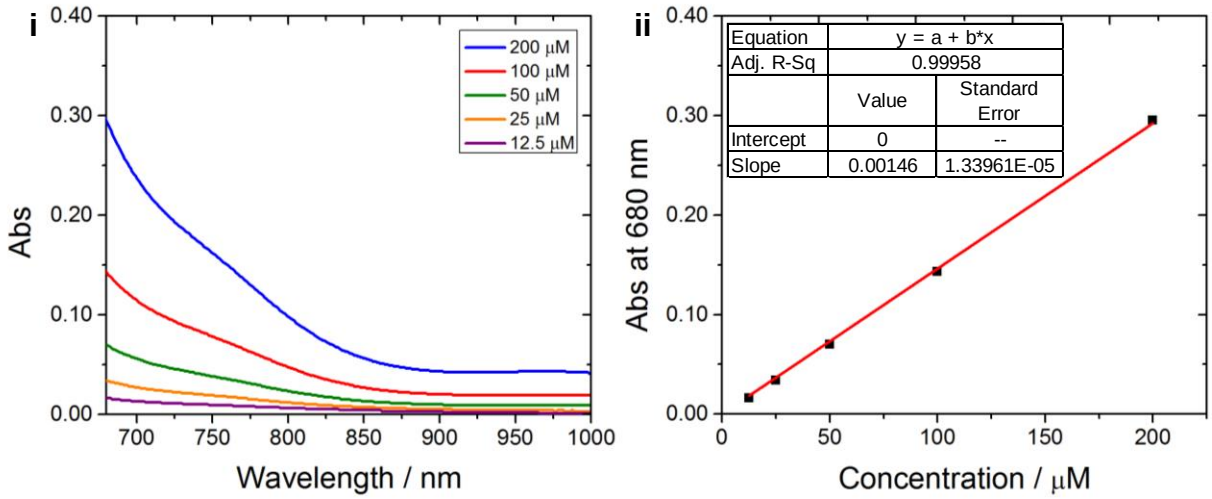

e) Cluster **8**

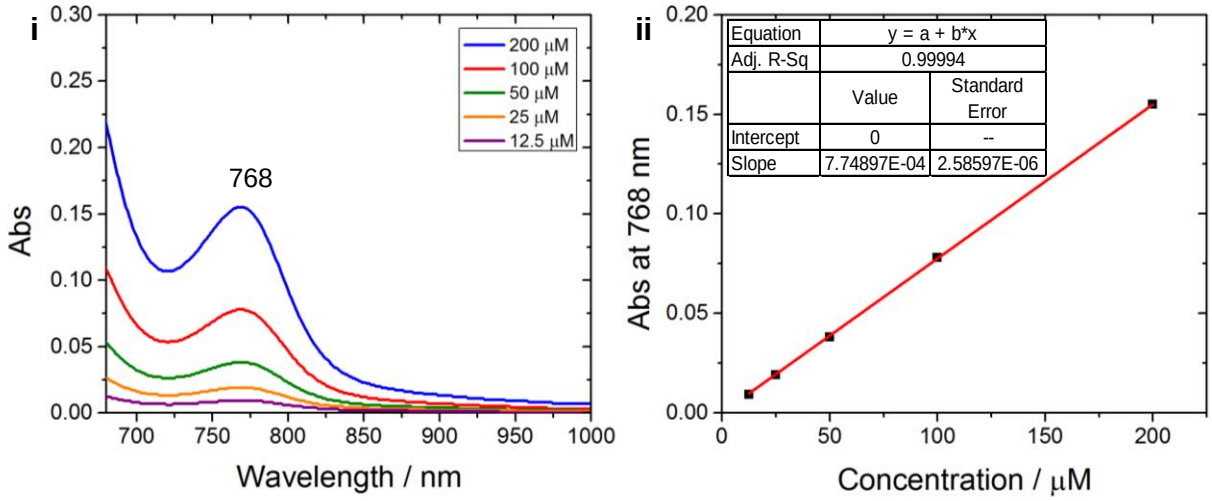

Figure S1 (cont'd). i) Optical absorption spectra of various concentrations (in DMSO), ii) plot of optical absorbance (at respective λ_{max}) as a function of concentrations of d) cluster **7** and e) cluster **8**.

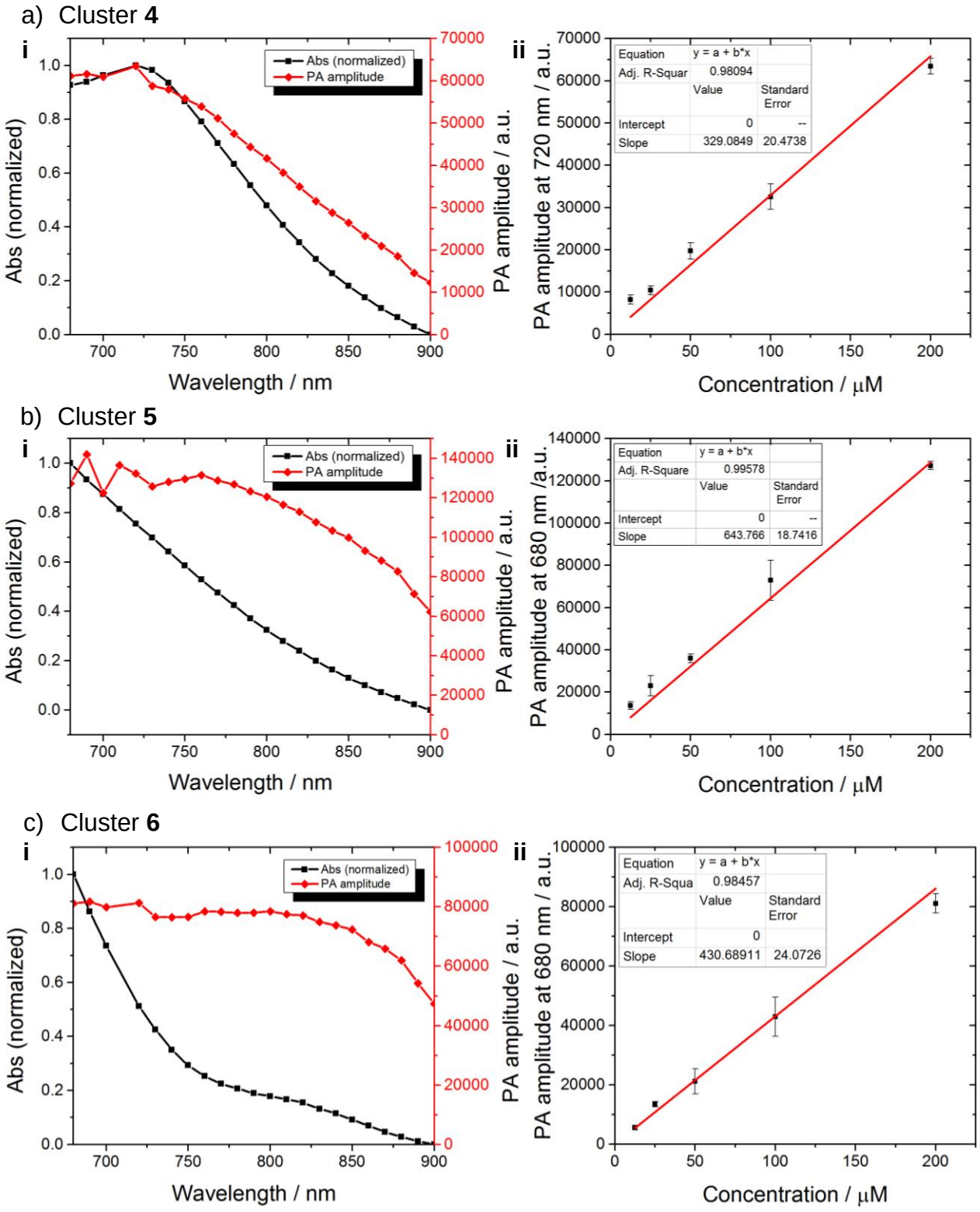

Figure S2. i) PA (red) and optical absorption (black) spectra, ii) PA amplitude as a function of concentration of a) cluster **4**, b) cluster **5** and c) cluster **6**.

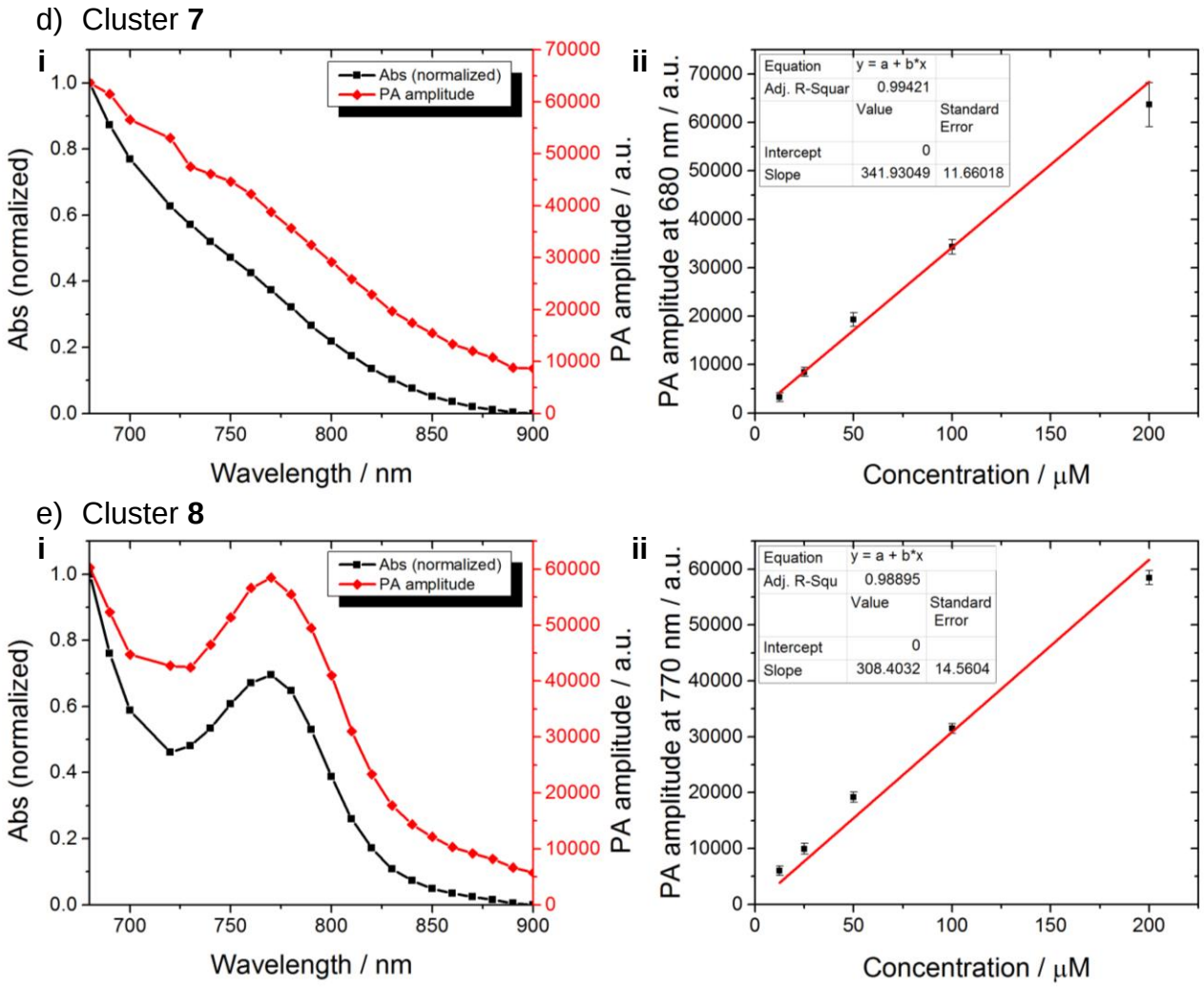

Figure S2 (cont'd). i) PA (red) and optical absorption (black) spectra, ii) plot of PA amplitude as a function of concentration of d) cluster **7** and e) cluster **8**.

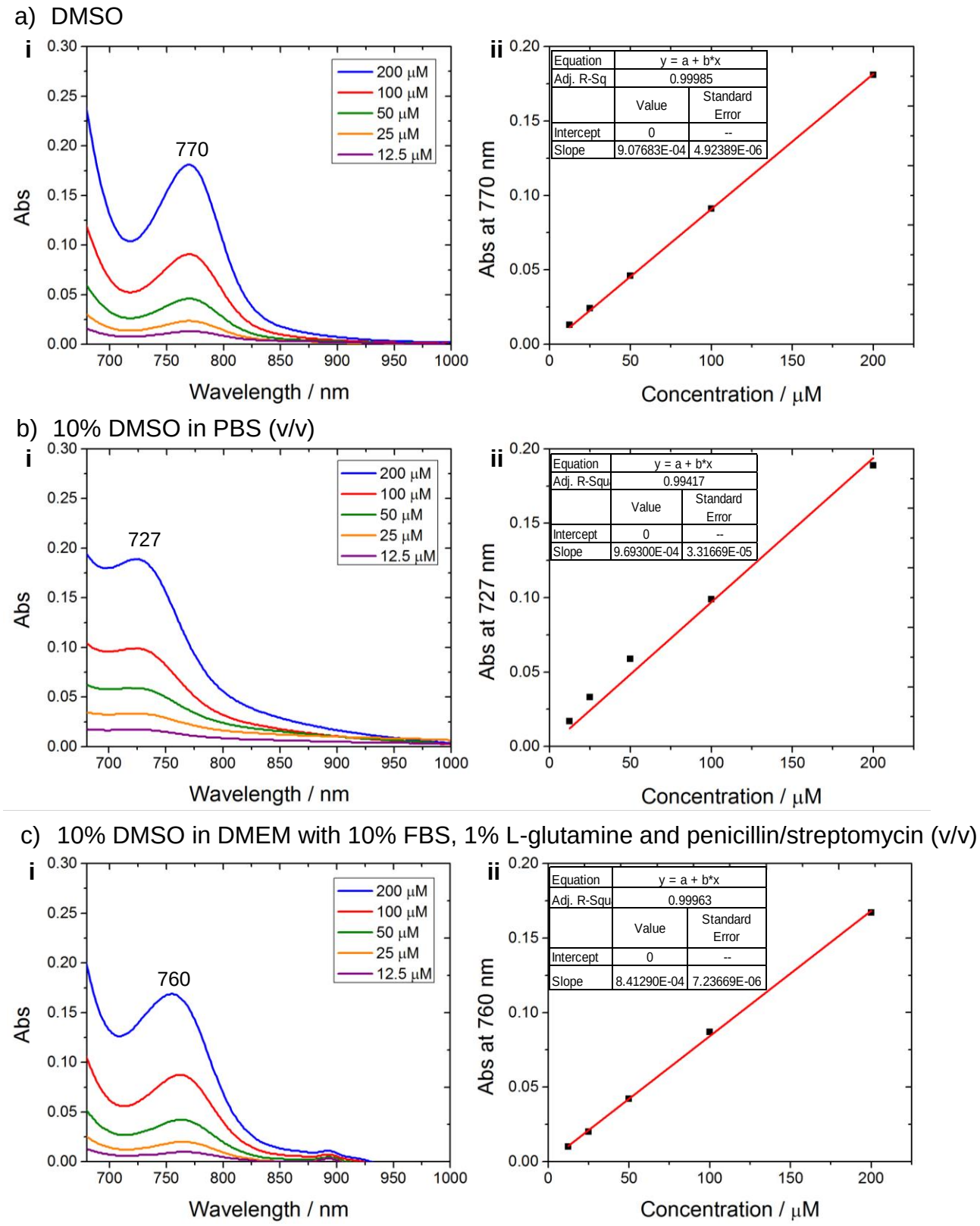

Figure S3. i) Optical absorption spectra of **9** of various concentrations and ii) plot of λ_{max} as a function of concentration of **9** in a) DMSO, b) 10% DMSO in PBS (v/v), and c) 10% DMSO in modified DMEM (v/v).

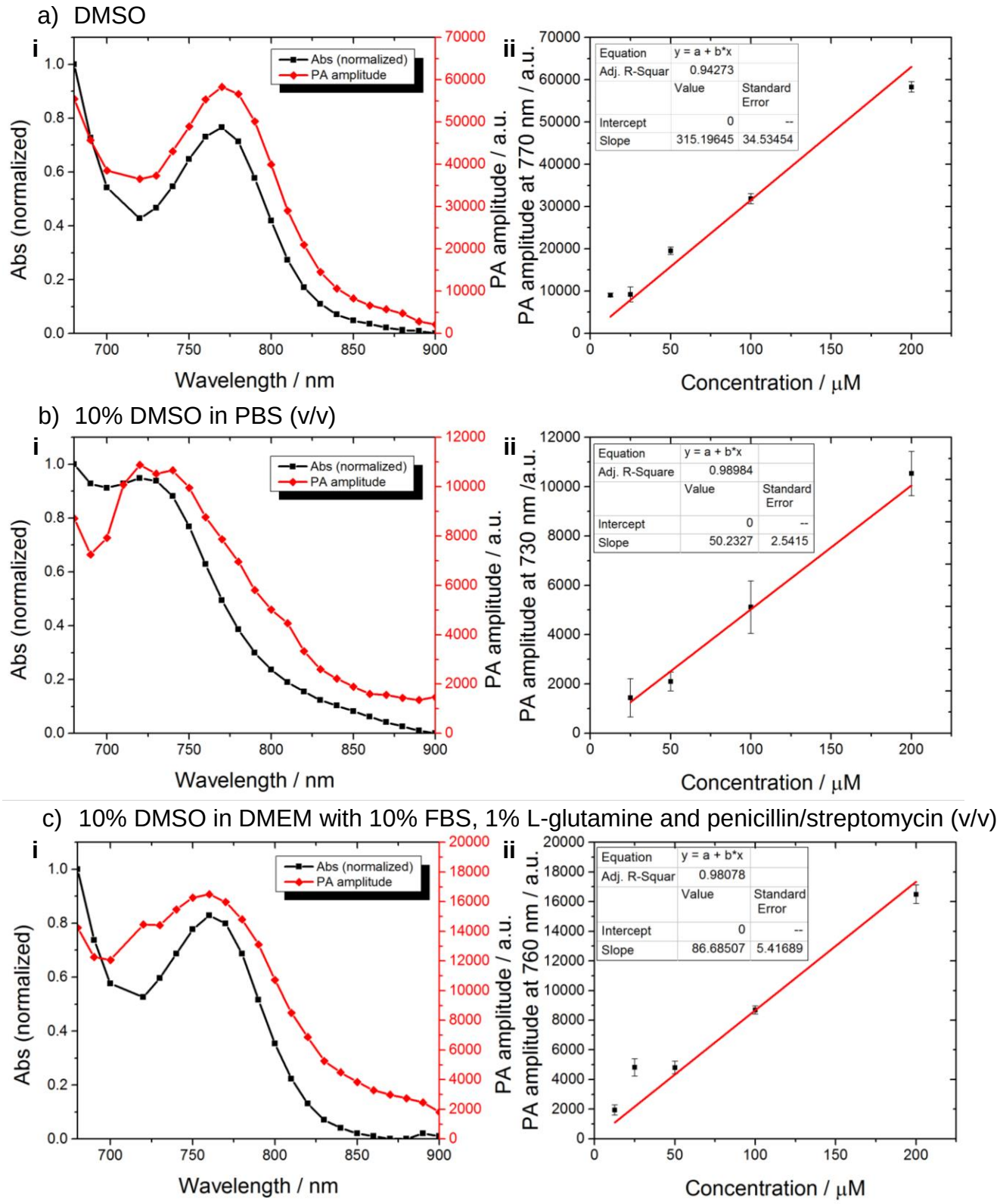

Figure S4. i) PA (red) and optical absorption (black) spectra of **9**, ii) plot of PA amplitude (at respective λ_{max}) as a function of concentration of **9** in a) DMSO, b) 10% DMSO in PBS (v/v), and c) 10% DMSO in modified DMEM (v/v).

a)

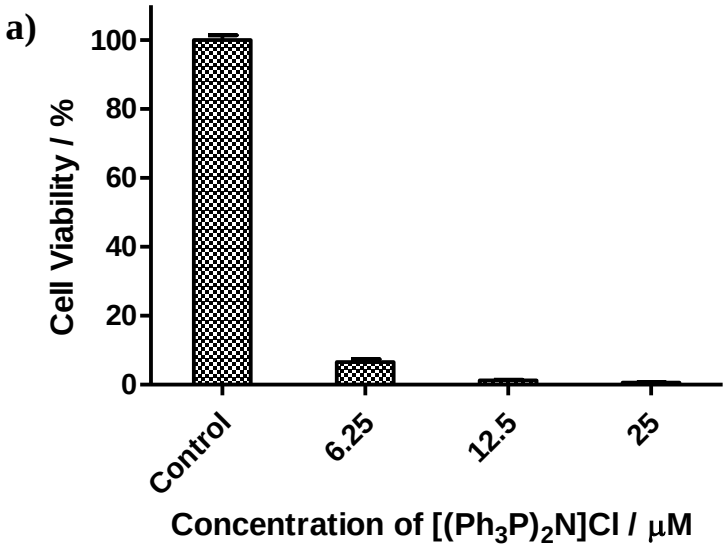

b)

Replicate 1 - MTS assay of $[(Ph_3P)_2N]Cl$ on OSCC cells

Concentration (C) / μM	Cell viability (V) / %	100-Y	X=ln C	Y=ln [V/(100-V)]	Y_0	X_0
25.0	0.60	99.40	3.22	-5.103	0	0.3773
12.5	1.21	98.79	2.53	-4.406	**IC_{50} =**	**1.46**
6.3	6.55	93.45	1.84	-2.657		

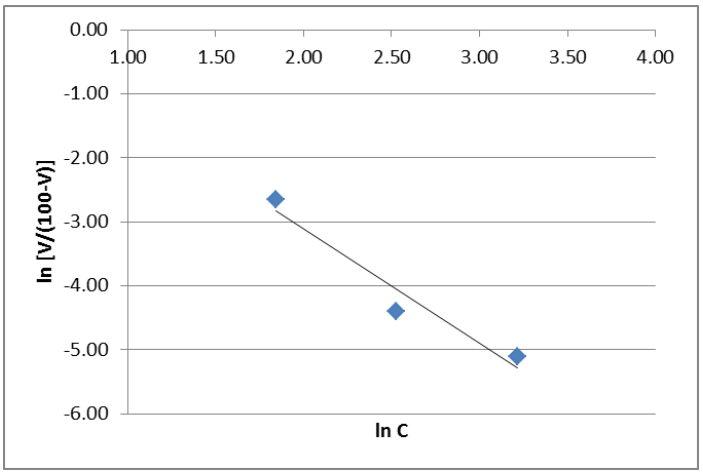

-0.5304402	0.3773
0.1336792	0.5593
0.9402810	0.2382
15.7450903	1
0.8931749	0.0567

Figure S5. a) First replicate of cell viability assay of $[(Ph_3P)_2N]Cl$ on OSCC cells, using 1 % DMSO as vehicle, b) calculation of IC_{50}.

c)

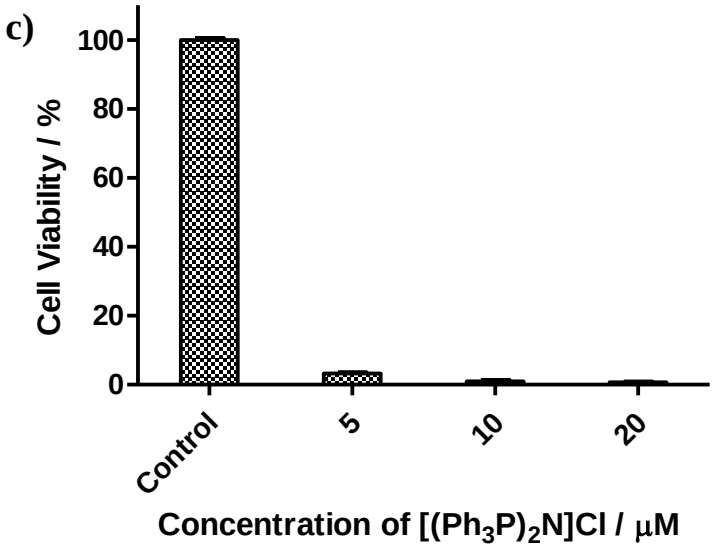

d)

Replicate 2 - MTS assay of $[(Ph_3P)_2N]Cl$ on OSCC cells

Concentration (C) / μM	Cell viability (V) / %	100-V	X=ln C	Y=ln [V/(100-V)]	Y_0	X_0
20.0	0.72	99.28	3.00	-4.923	0	-1.1710
10.0	0.96	99.04	2.30	-4.635	**IC_{50} =**	**0.31**
5.0	3.24	96.76	1.61	-3.397		

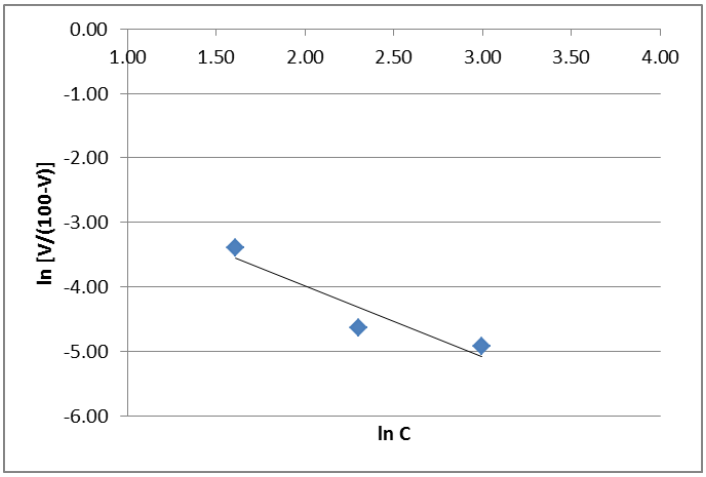

-0.8043229	-1.1710
0.2890845	1.2630
0.8855999	0.3316
7.7412536	1
0.8509783	0.1099

Figure S5 (cont'd). c) Second replicate of cell viability assay of $[(Ph_3P)_2N]Cl$ on OSCC cells, using 1 % DMSO as vehicle, d) calculation of IC_{50}.

e)

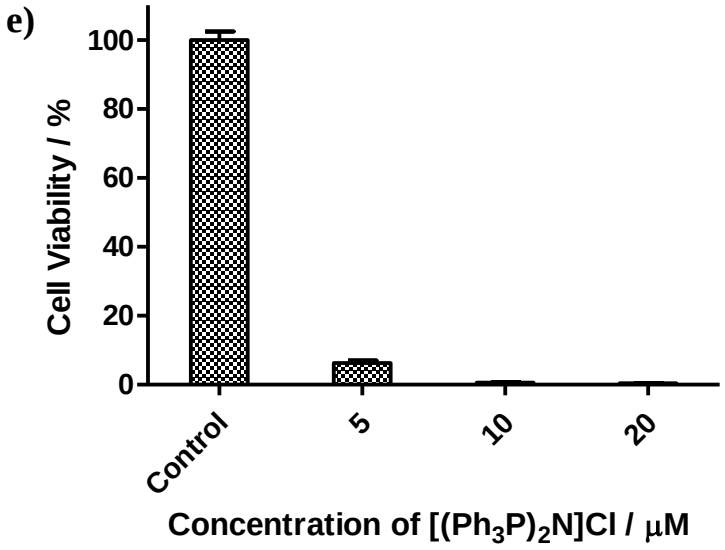

f)

Replicate 3 - MTS assay of $[(Ph_3P)_2N]Cl$ on OSCC cells

Concentration (C) / μM	Cell viability (V) / %	100-V	X=ln C	Y=ln [V/(100-V)]	Y_0	X_0
20.0	0.40	99.60	3.00	-5.511	0	0.4231
10.0	0.62	99.38	2.30	-5.083	**IC_{50} =**	**1.53**
5.0	6.32	93.68	1.61	-2.697		

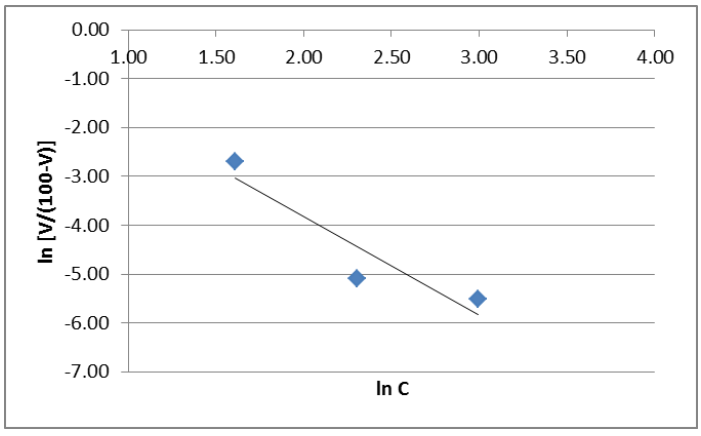

-0.4242441	0.4231
0.1703612	0.7836
0.8611382	0.3653
6.2014057	1
0.8274729	0.1334

Mean IC_{50}	**1.10**
Standard error	0.40

Figure S5 (cont'd). e) Third replicate of cell viability assay of $[(Ph_3P)_2N]Cl$ on OSCC cells, using 1 % DMSO as vehicle, f) calculation of IC_{50} and the mean value from three replicates.

a)

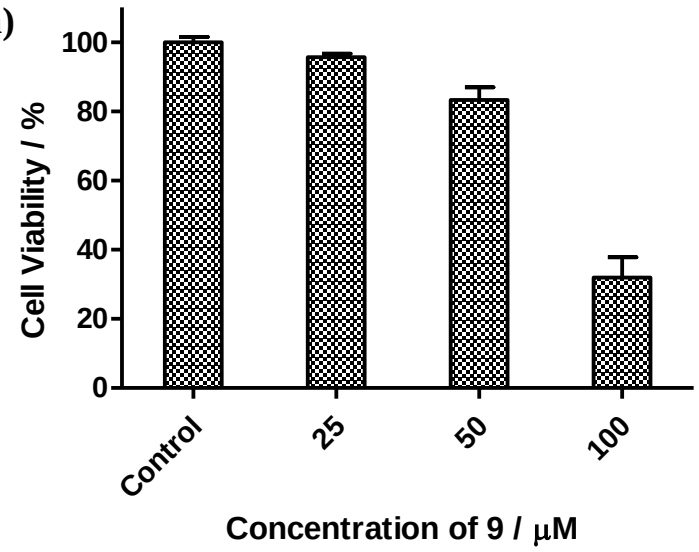

b)

Replicate 1 - MTS assay of $Na_2[Os_{10}(\mu_6\text{-}C)(CO)_{24}]$ (9) on OSCC cells

Concentration (C) / μM	Cell viability (V) / %	100-V	X=ln C	Y=ln [V/(100-V)]	Y_0	X_0
100.0	31.91	68.09	4.61	-0.758	0	4.3773
50.0	83.32	16.68	3.91	1.609	**IC_{50}=**	**79.62**
25.0	95.69	4.31	3.22	3.099		

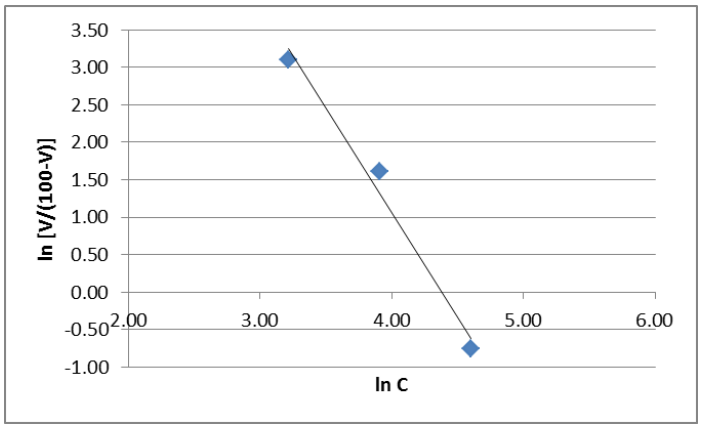

-0.3533478	4.3773
0.0463439	0.0956
0.9830888	0.1275
58.1325284	1
0.9446560	0.0163

Figure S6. a) First replicate of cell viability assay of $Na_2[Os_{10}(\mu_6\text{-}C)(CO)_{24}]$ (**9**) on OSCC cells, using 1 % DMSO as vehicle, b) calculation of IC_{50}.

c)

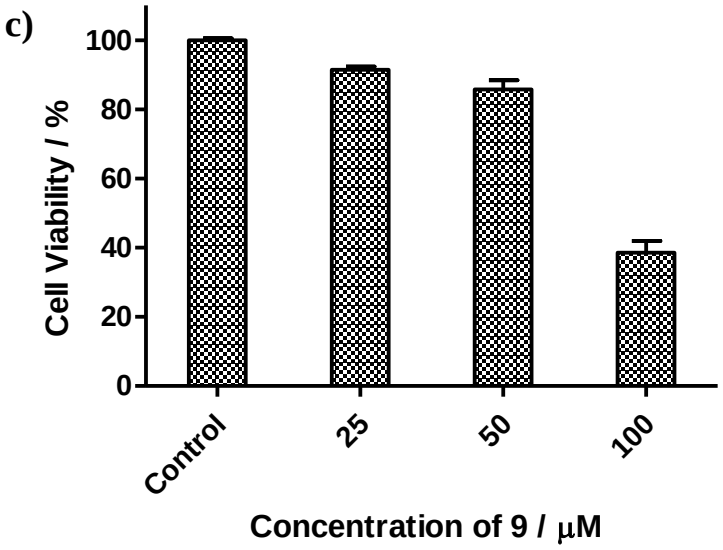

d)

Replicate 2 - MTS assay of $Na_2[Os_{10}(\mu_6\text{-}C)(CO)_{24}]$ (9) on OSCC cells

Concentration (C) / μM	Cell viability (V) / %	100-V	X=ln C	Y=ln [V/(100-V)]	Y_0	X_0
100.0	38.58	61.42	4.61	-0.465	0	4.4513
50.0	85.77	14.23	3.91	1.796	IC_{50}=	**85.73**
25.0	91.41	8.59	3.22	2.364		

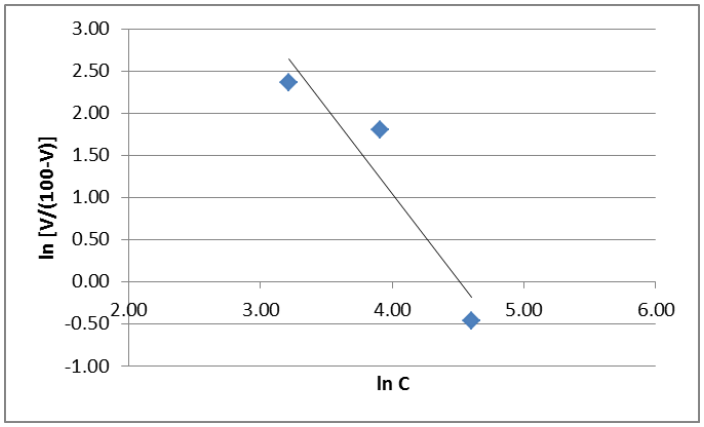

-0.4377199	4.4513
0.1513021	0.2625
0.8932715	0.3202
8.3695677	1
0.8583500	0.1026

Figure S6 (cont'd). c) Second replicate of cell viability assay of $Na_2[Os_{10}(\mu_6\text{-}C)(CO)_{24}]$ (**9**) on OSCC cells, using 1 % DMSO as vehicle, d) calculation of IC_{50}.

e)

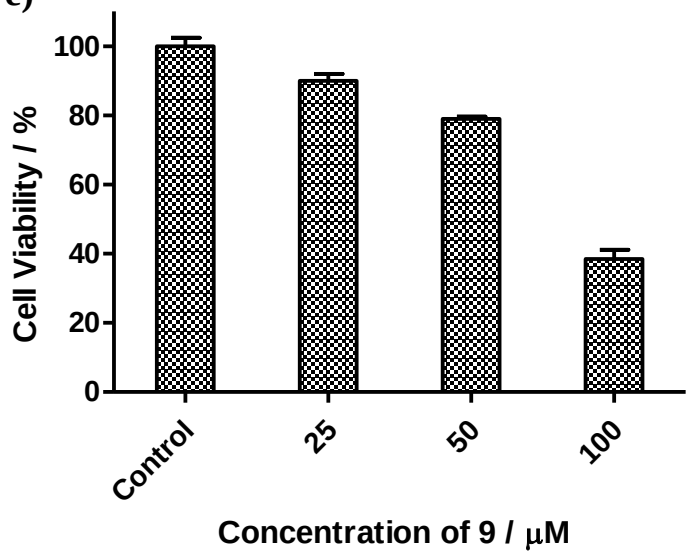

f)

Replicate 3 - MTS assay of $Na_2[Os_{10}(\mu_6\text{-}C)(CO)_{24}]$ (9) on OSCC cells

Concentration (C) / μM	Cell viability (V) / %	100-V	X=ln C	Y=ln [V/(100-V)]	Y_0	X_0
100.0	38.47	61.53	4.61	-0.470	0	4.4205
50.0	78.99	21.01	3.91	1.324	**IC_{50}=**	**83.14**
25.0	89.95	10.05	3.22	2.192		

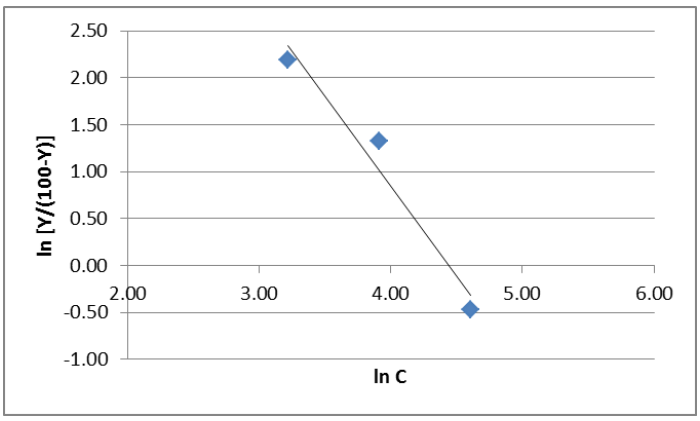

-0.5006497	4.4205
0.1005357	0.1511
0.9612382	0.1930
24.7986260	1
0.9236596	0.0372

Mean IC_{50}	**82.83**
Standard error	1.77

Figure S6 (cont'd). e) Third replicate of cell viability assay of $Na_2[Os_{10}(\mu_6\text{-}C)(CO)_{24}]$ (**9**) on OSCC cells, using 1 % DMSO as vehicle, f) calculation of IC_{50} and the mean value from three replicates.

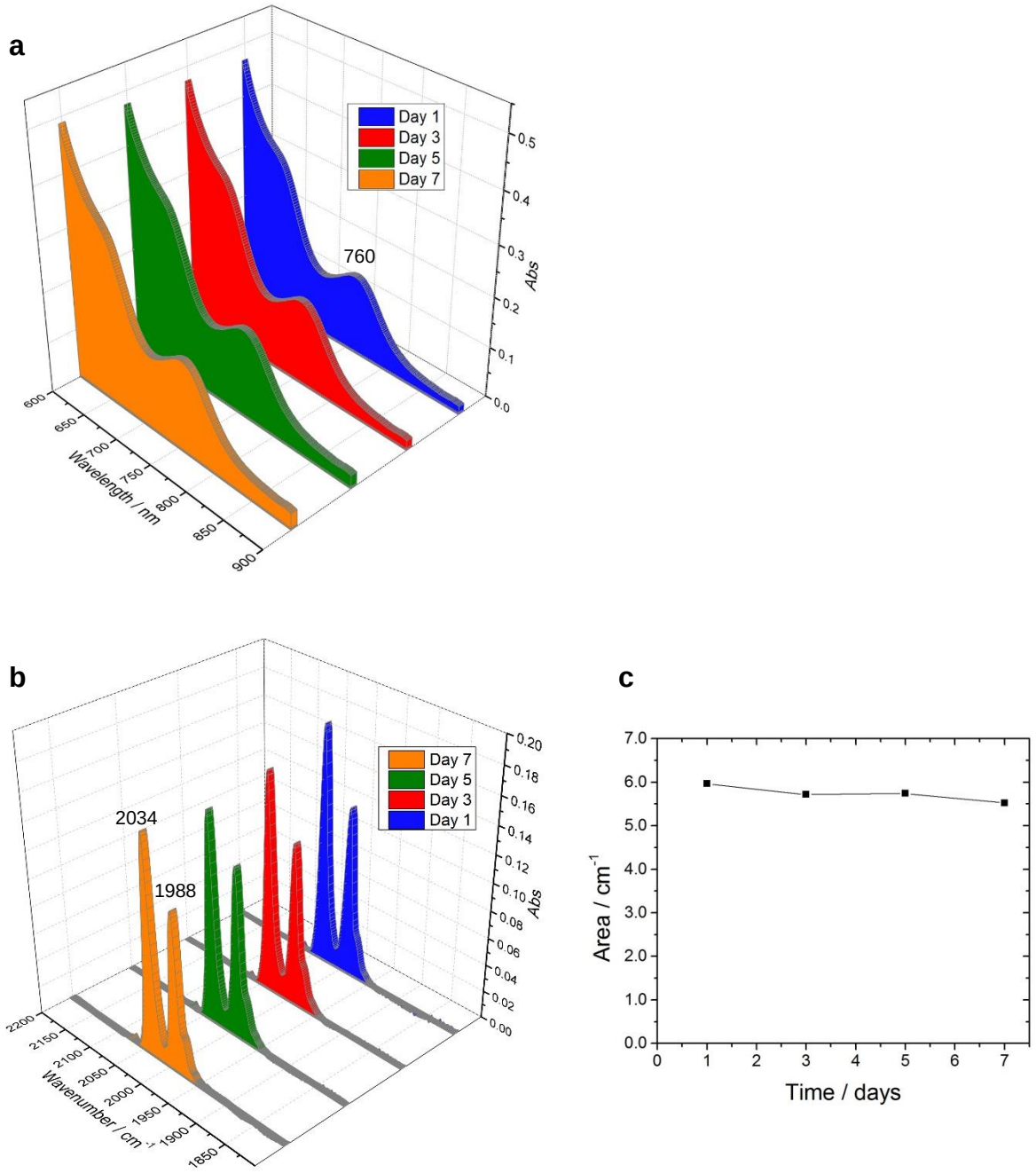

Figure S7. Time course study of a solution of **9** (200 μM) in 10% DMSO in modified DMEM, over a period of 7 days: a) Optical absorption spectra, b) FTIR spectra (νCO) obtained from the dried samples and b) integrals of the νCO absorbance.

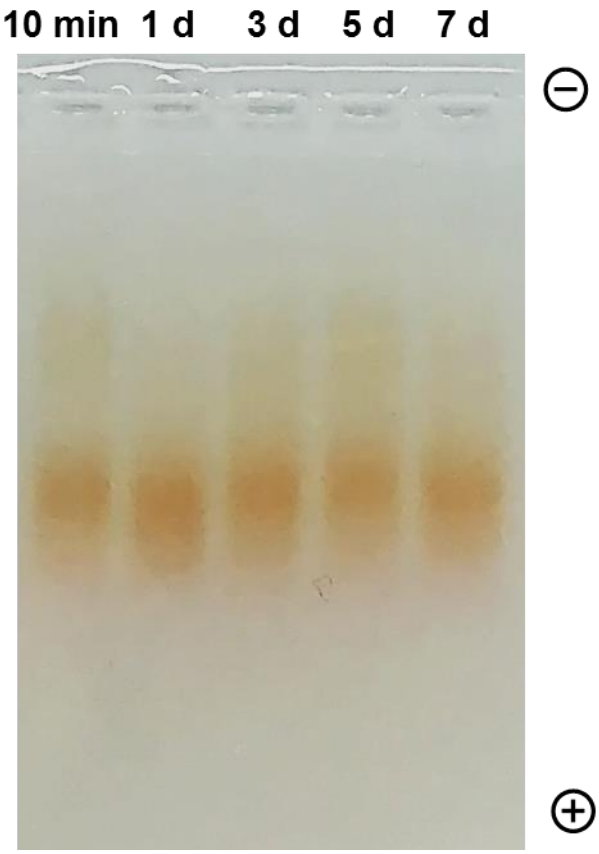

Figure S8. True color photograph of cluster **9** (200 μM) electrophoresed through 1% agarose gel for 30 min at 150 V (15 cm electrode spacing) in 0.5 x TAE buffer. The five lanes contain cluster **9** (200 μM) in 10% DMSO in modified DMEM incubated for 10 min, 1, 3, 5 and 7 days respectively prior to the gel electrophoresis.

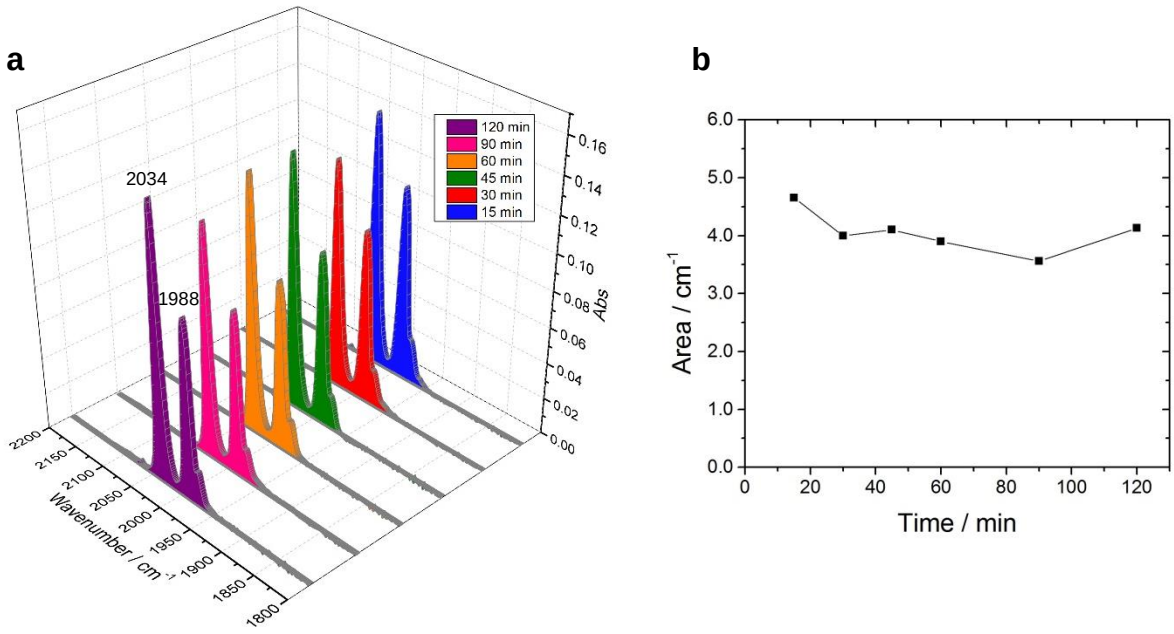

Figure S9. Irradiation of a solution of **9** (200 μM) in 10% DMSO in modified DMEM at 760 nm for various time intervals: a) FTIR spectra (ν_{CO}) obtained from the dried samples, and b) integrals of the ν_{CO} absorbance.

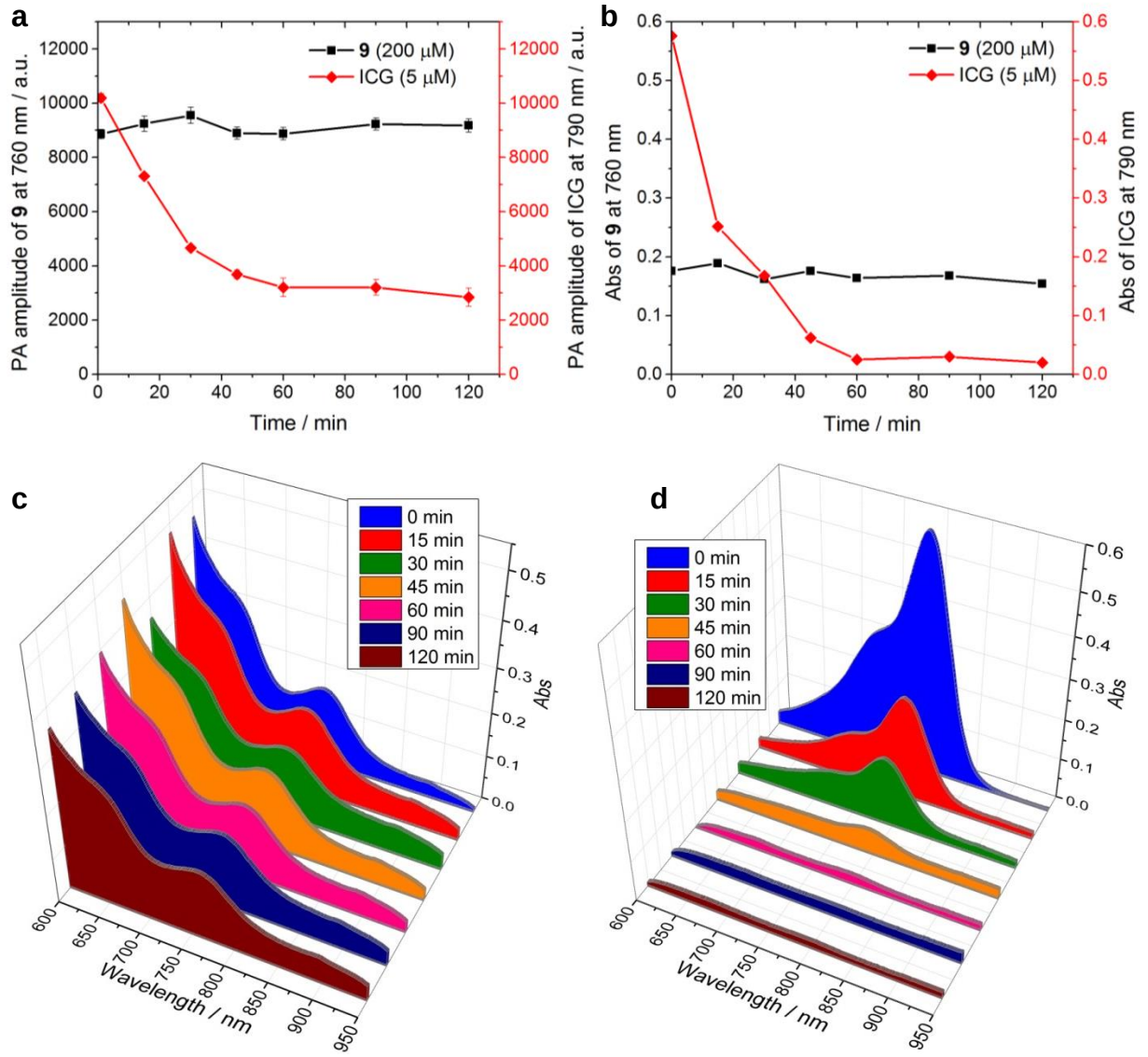

Figure S10. Time course studies of **9** and ICG over 120 min with irradiation at the respective λ_{max}: a) PA amplitude as a function of time, b) optical absorbance as a function of time, c) optical absorption spectra of **9** and d) ICG.

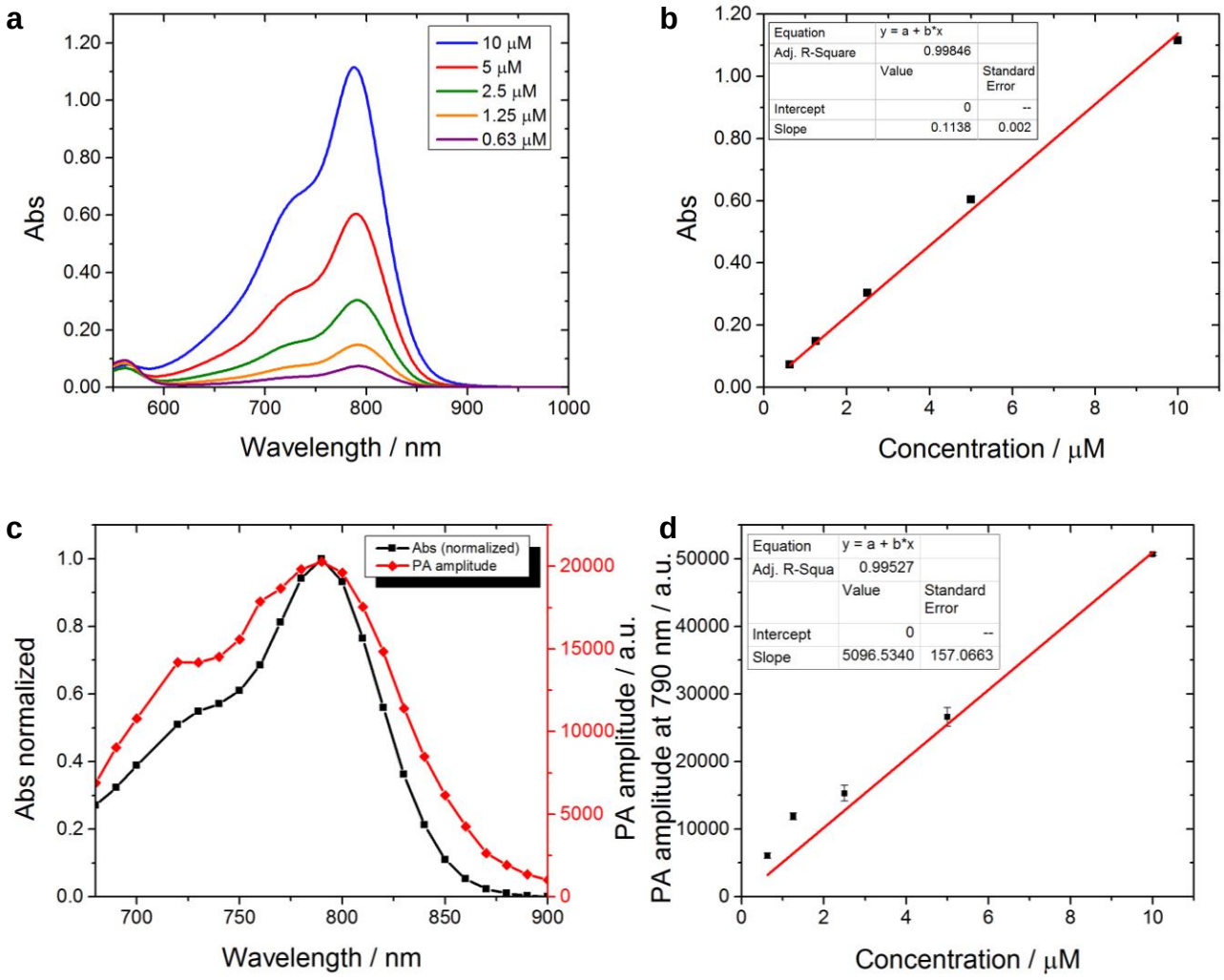

Figure S11 a) Optical absorption spectra of ICG of various concentrations, b) plot of absorbance of ICG at $\lambda_{max=}$790 nm as a function of concentration, c) PA (red) and optical absorption (black) spectra of ICG, d) plot of PA amplitude at $\lambda_{max=}$790 nm as a function of concentration of ICG in 10% DMSO in modified DMEM (v/v).

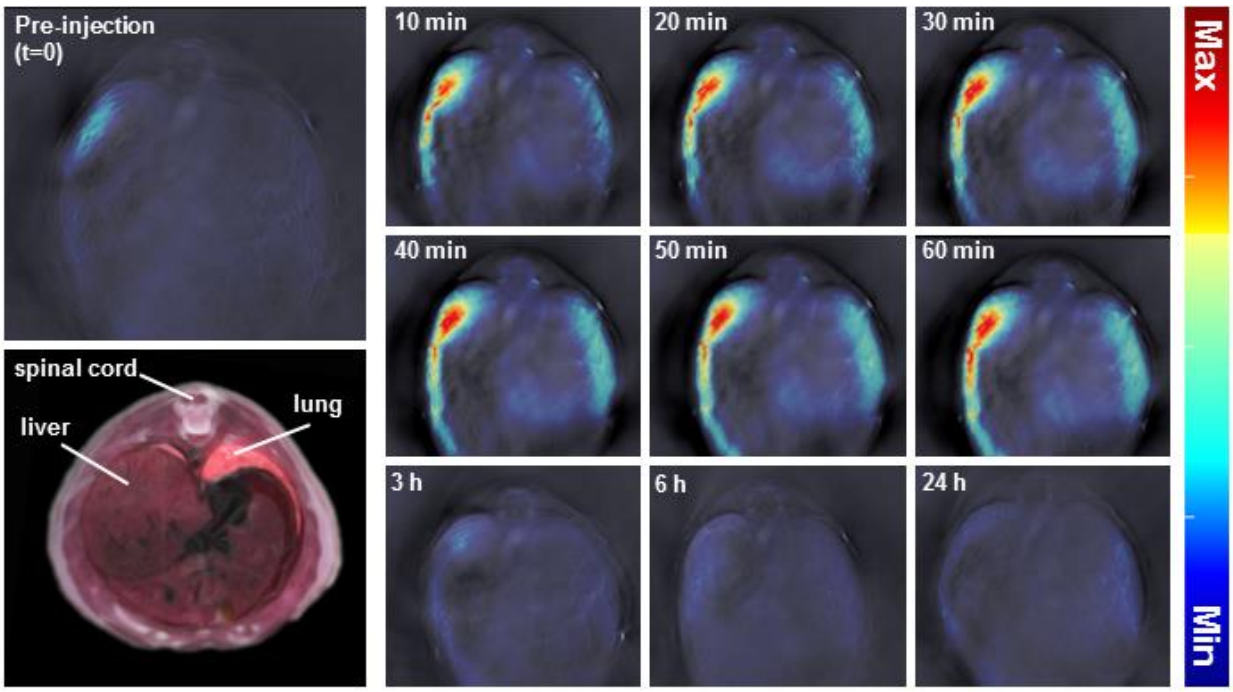

Figure S12. *In vivo* PA imaging of mouse OSCC xenograft model using **9** as a contrast agent. PA signal from **9** across a single slice of the mouse abdomen showing liver before and after injection up to 24 h. All PA images are overlaid on their corresponding anatomy images at 800 nm. Bottom left corner shows the reference anatomy of a single abdominal slice depicting in particular, the liver of a frozen sectioned mouse, as obtained elsewhere.[11]

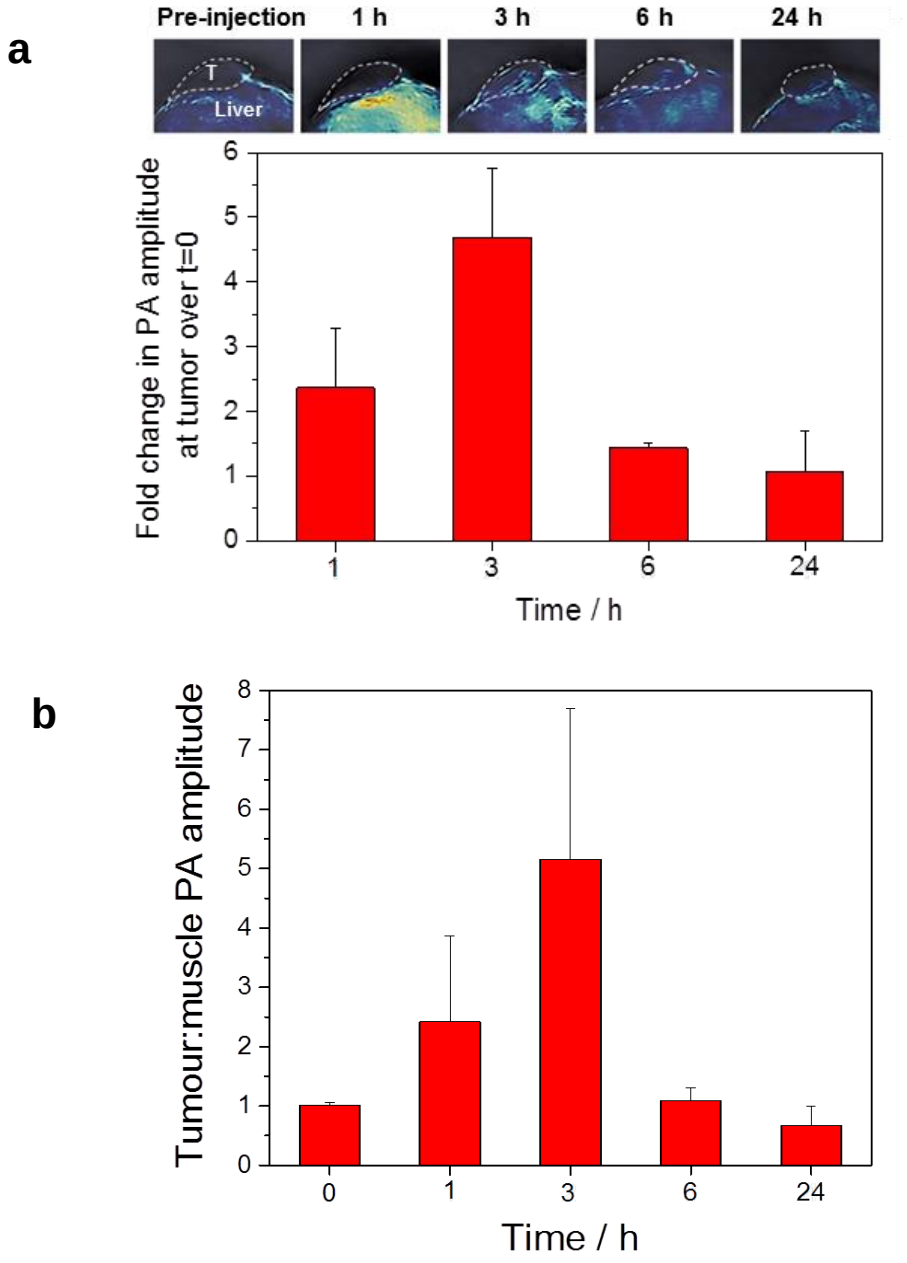

Figure S13. a) Enlarged images of the tumors at various time point with the PA intensities normalized (top). Fold change in PA intensity in the tumor over that at t=0 in the tumor (bottom). Error bars represent standard error of the mean, n = 3. b) Tumor-to-muscle ratio of PA amplitude at various time points up till 24 h. Error bars represent standard error of the mean, n = 3.

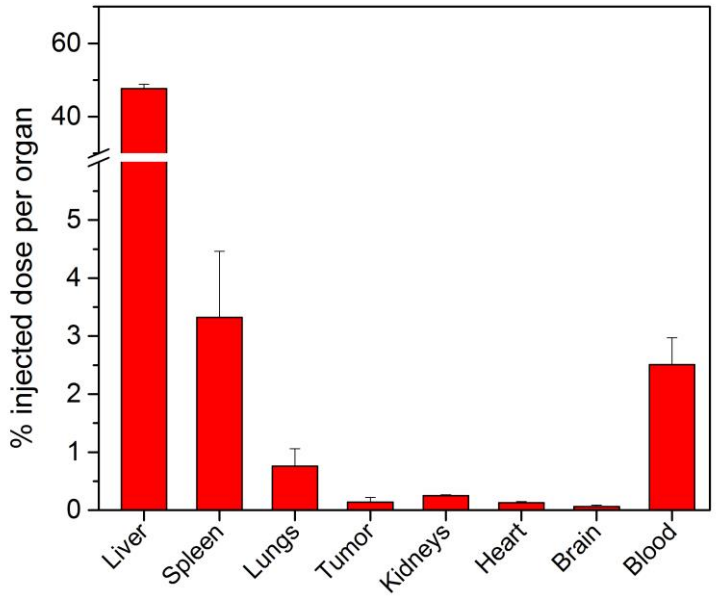

Figure S14. ICP-MS analysis of the percentage retention of injected dose (% ID) of **9** per organs, 24 h after injection. Error bars represent standard error of the mean, n = 3.

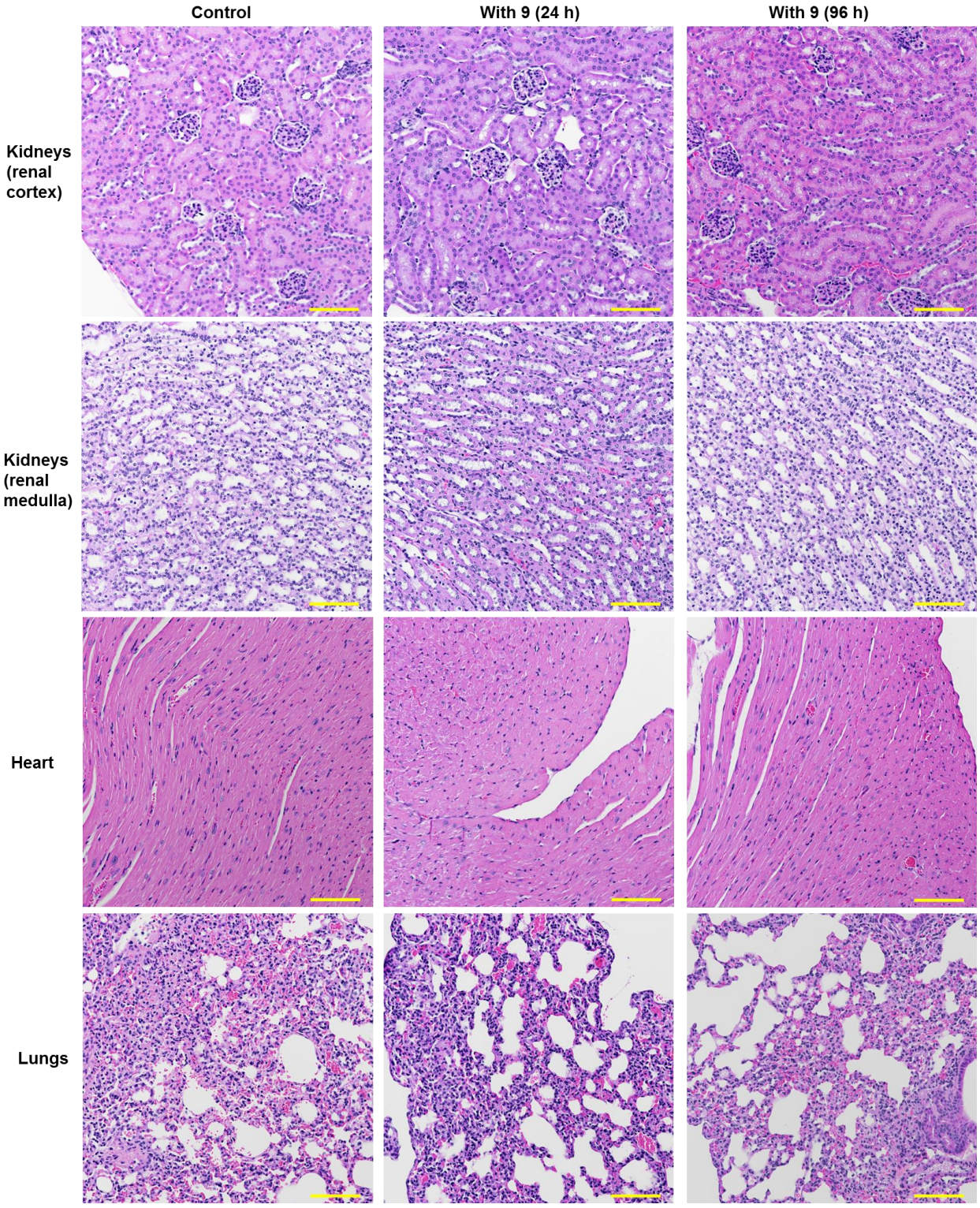

Figure S15. Histopathology (H & E staining) of kidneys, heart and lungs tissues of mice, 24 h and 96 h after intravenous injection of **9**, with that of control samples. Scale bar = 100 μm.

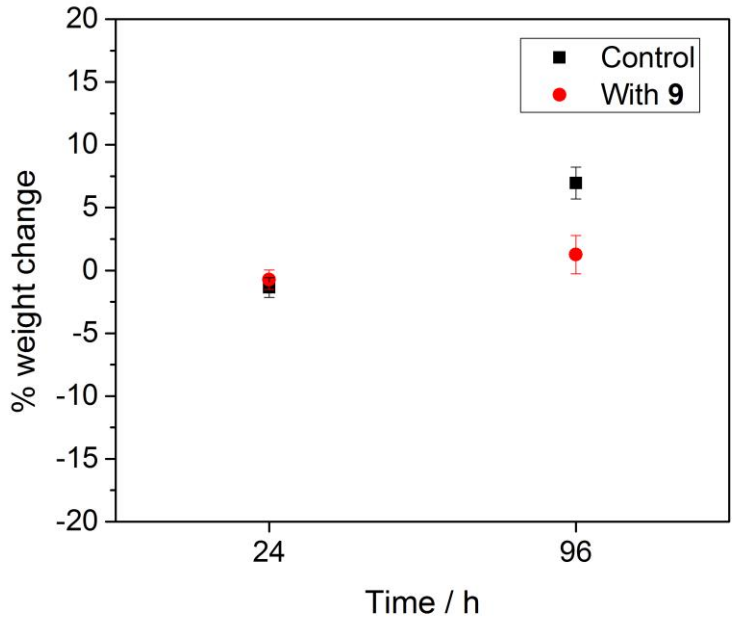

Figure S16. Percentage weight change of control mice and mice injected with **9** up till 24 h and 96 h with respect to initial weight. Error bars represent standard error of the mean, n = 3 for samples with **9** and n = 2 for control samples.

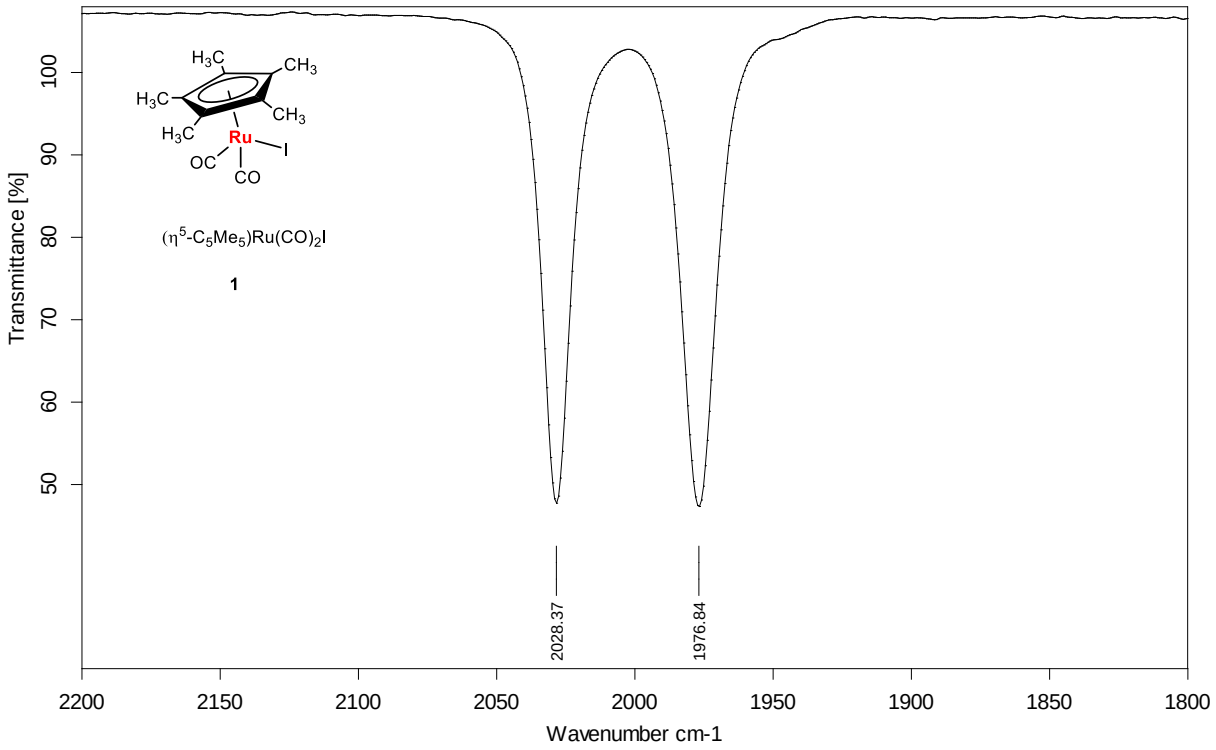

Figure S17. IR spectrum (ν_{CO}) of **1** in DCM.

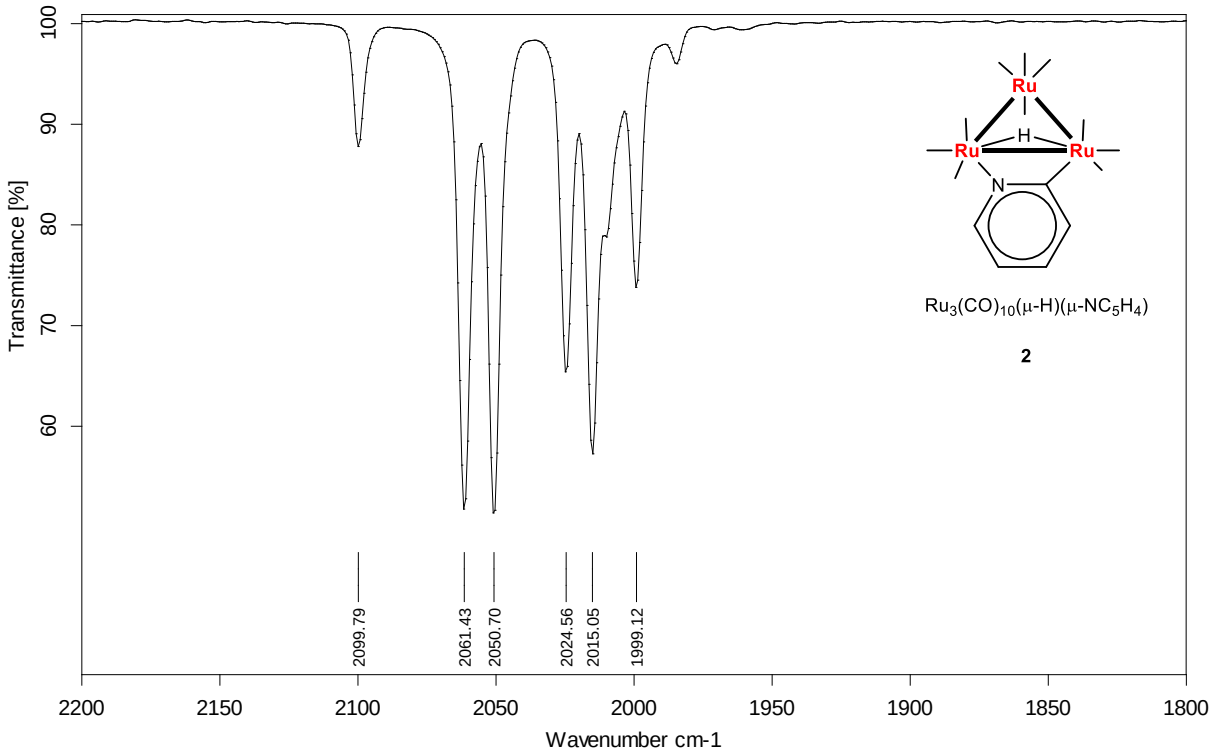

Figure S18. IR spectrum (ν_{CO}) of cluster **2** in hexane.

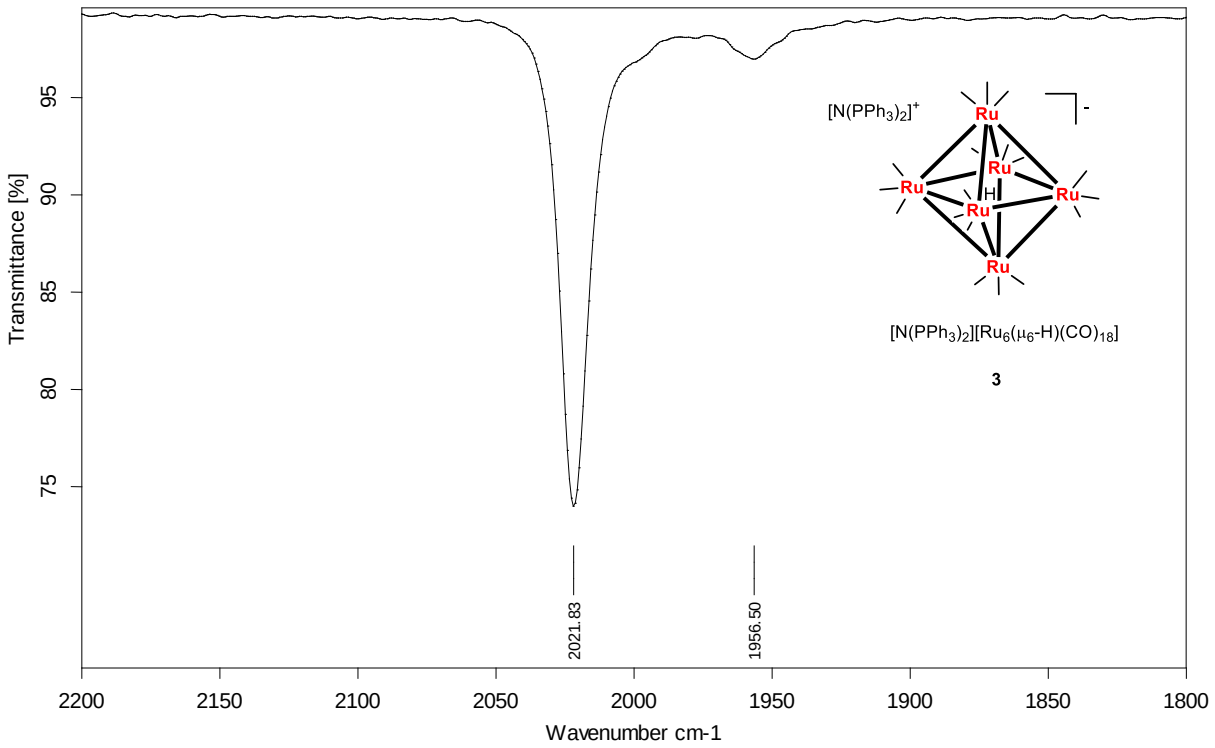

Figure S19. IR spectrum (ν_{CO}) of cluster **3** in DCM.

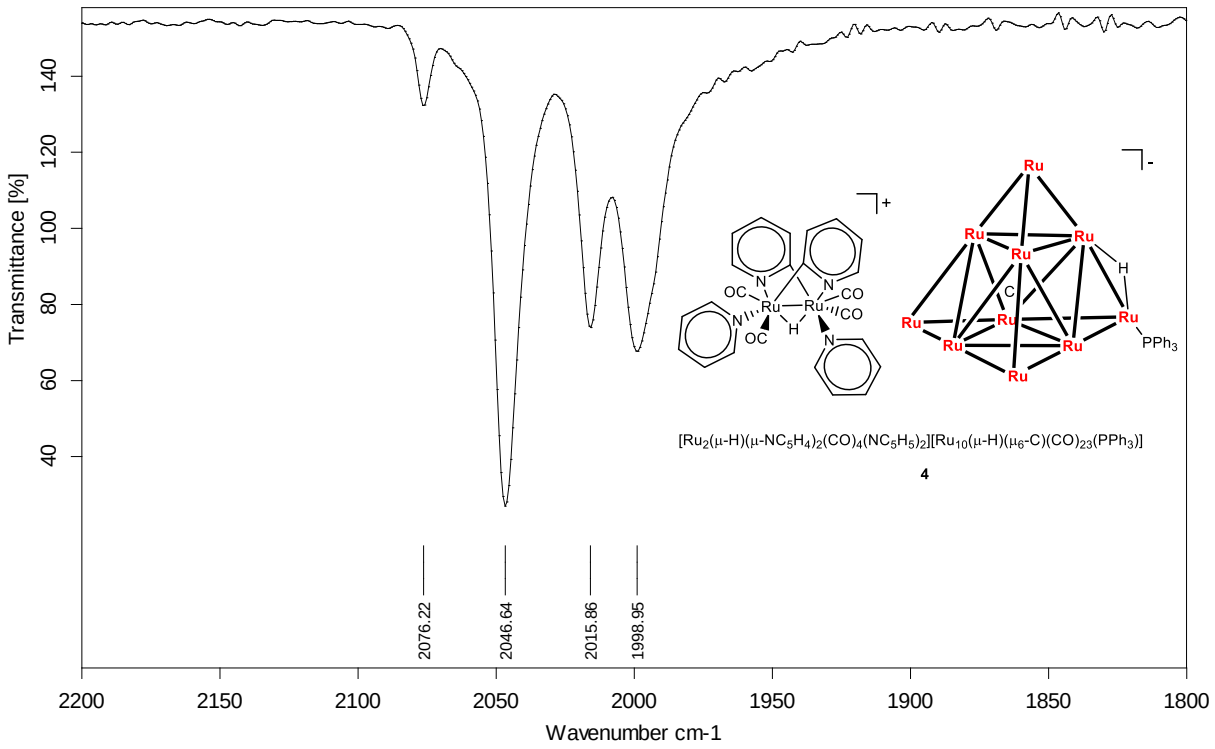

Figure S20. IR spectrum (ν_{CO}) of cluster **4** in DCM.

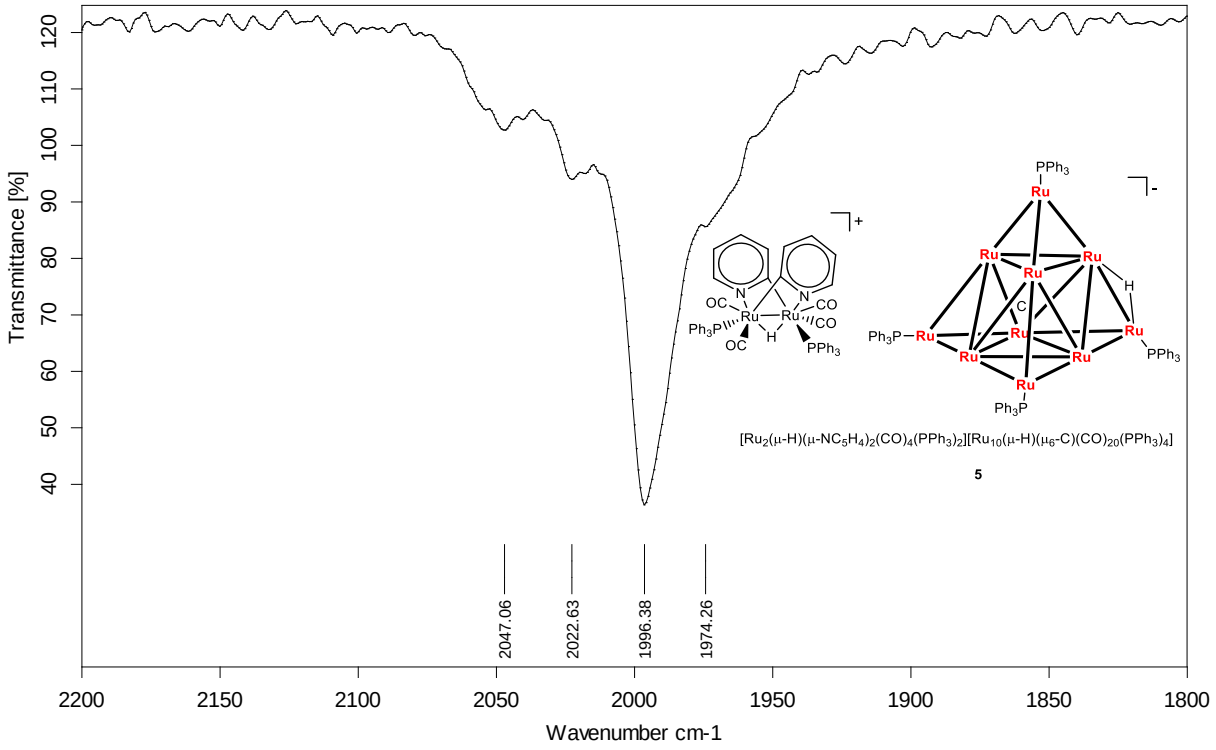

Figure S21. IR spectrum (ν_{CO}) of cluster **5** in DCM.

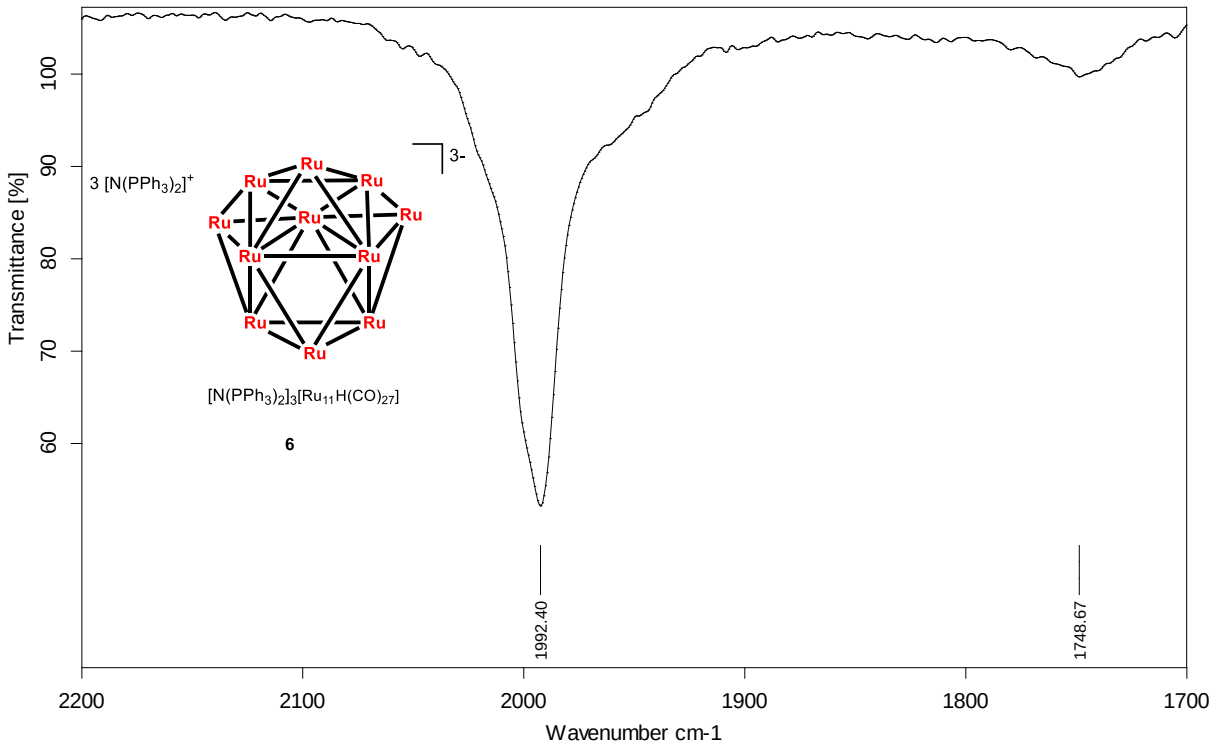

Figure S22. IR spectrum (ν_{CO}) of cluster **6** in DCM.

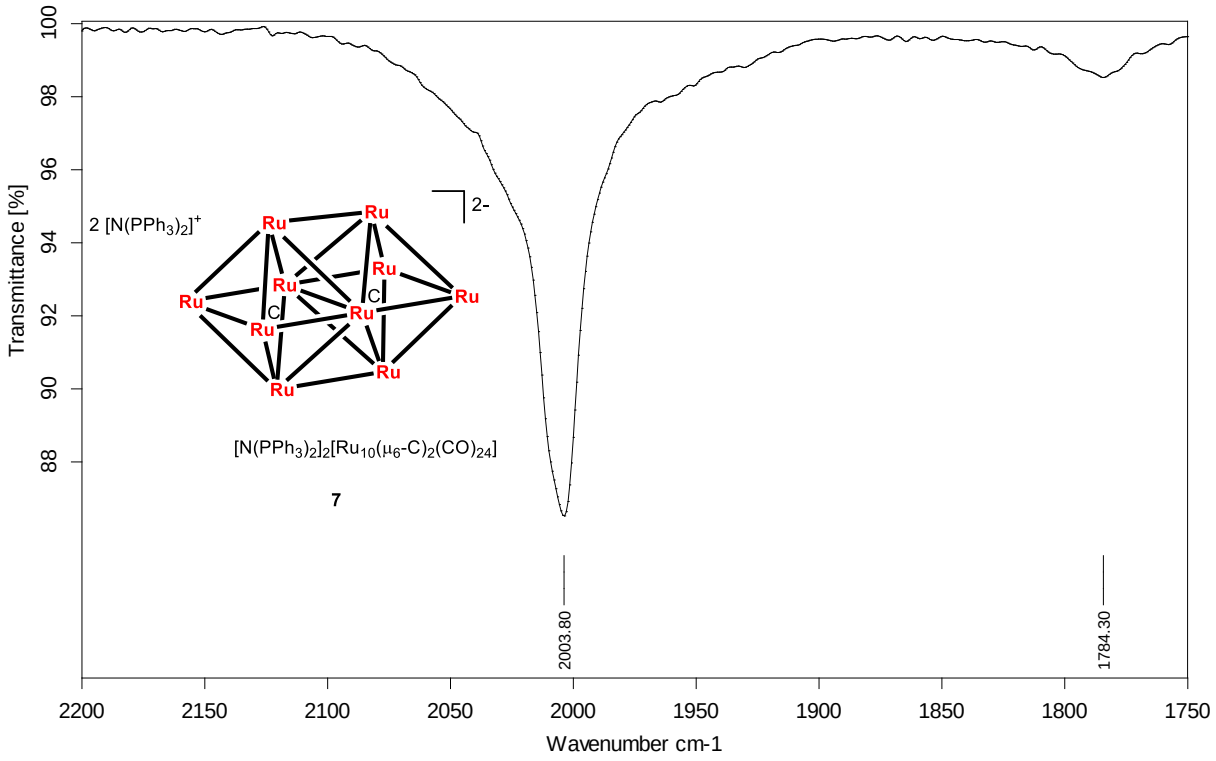

Figure S23. IR spectrum (ν_{CO}) of cluster **7** in DCM.

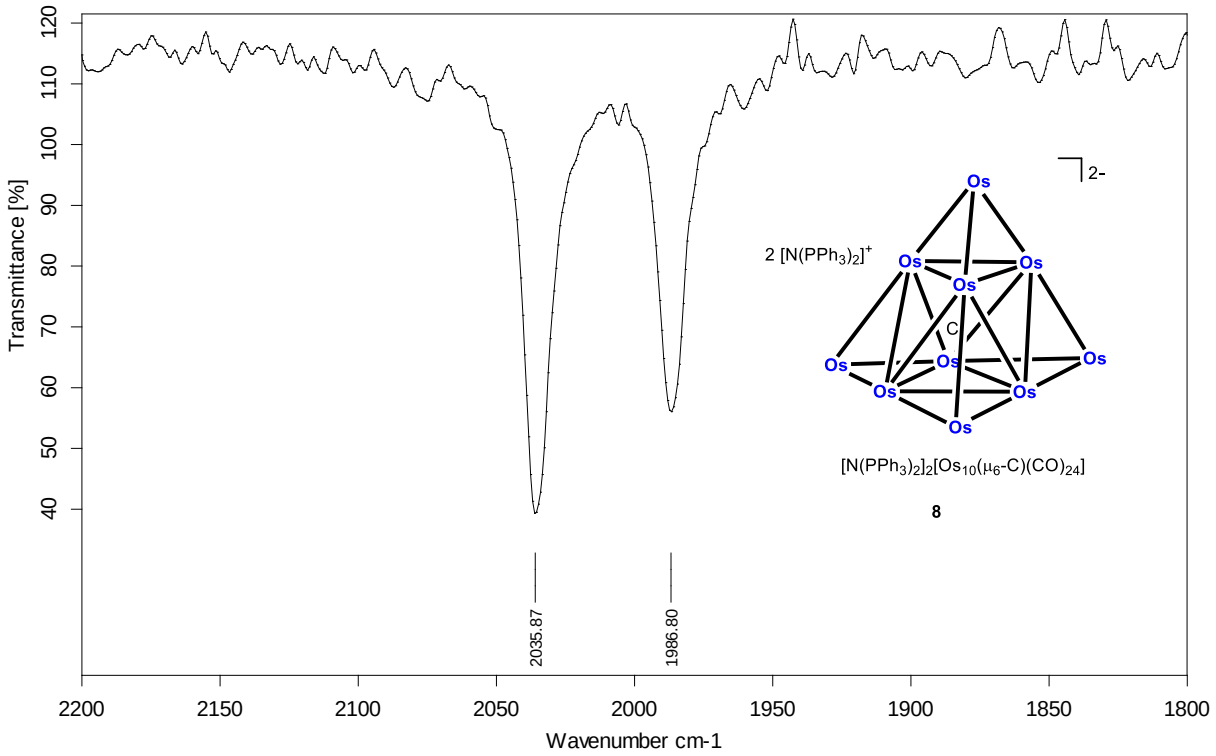

Figure S24. IR spectrum (ν_{CO}) of cluster **8** in DCM.

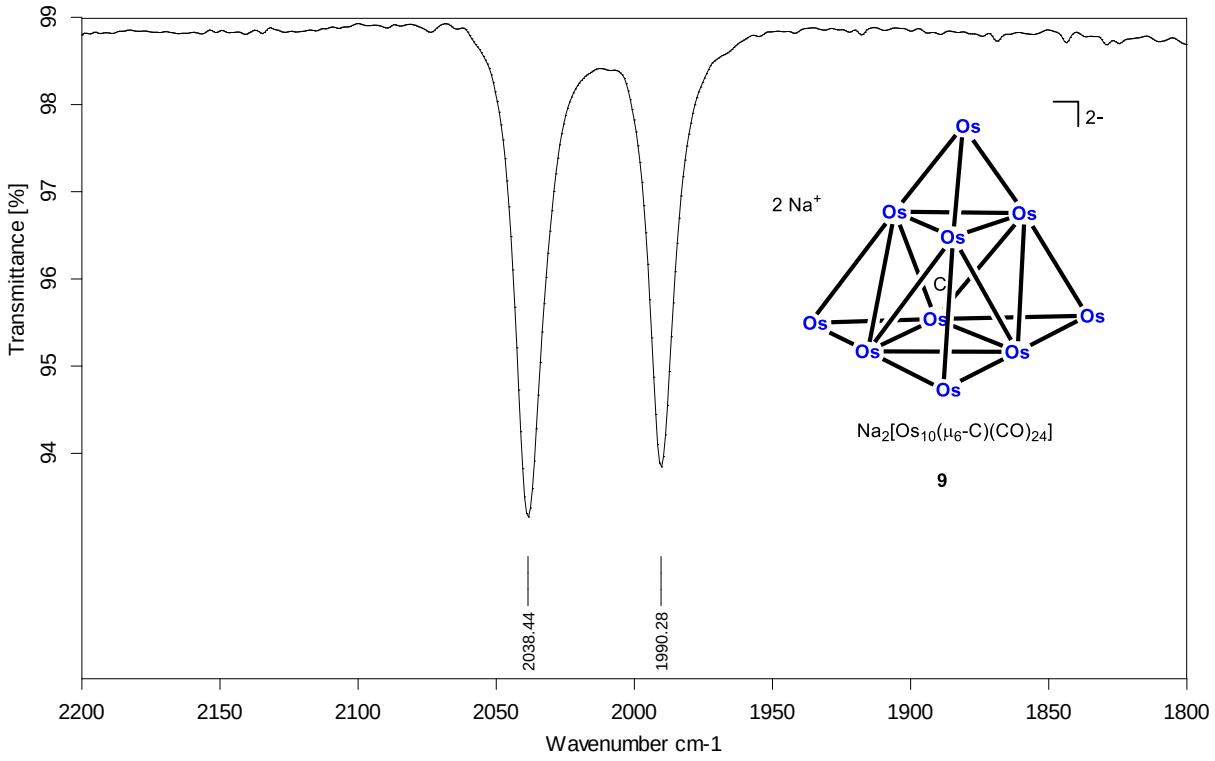

Figure S25. IR spectrum (ν_{CO}) of cluster **9** in acetonitrile.

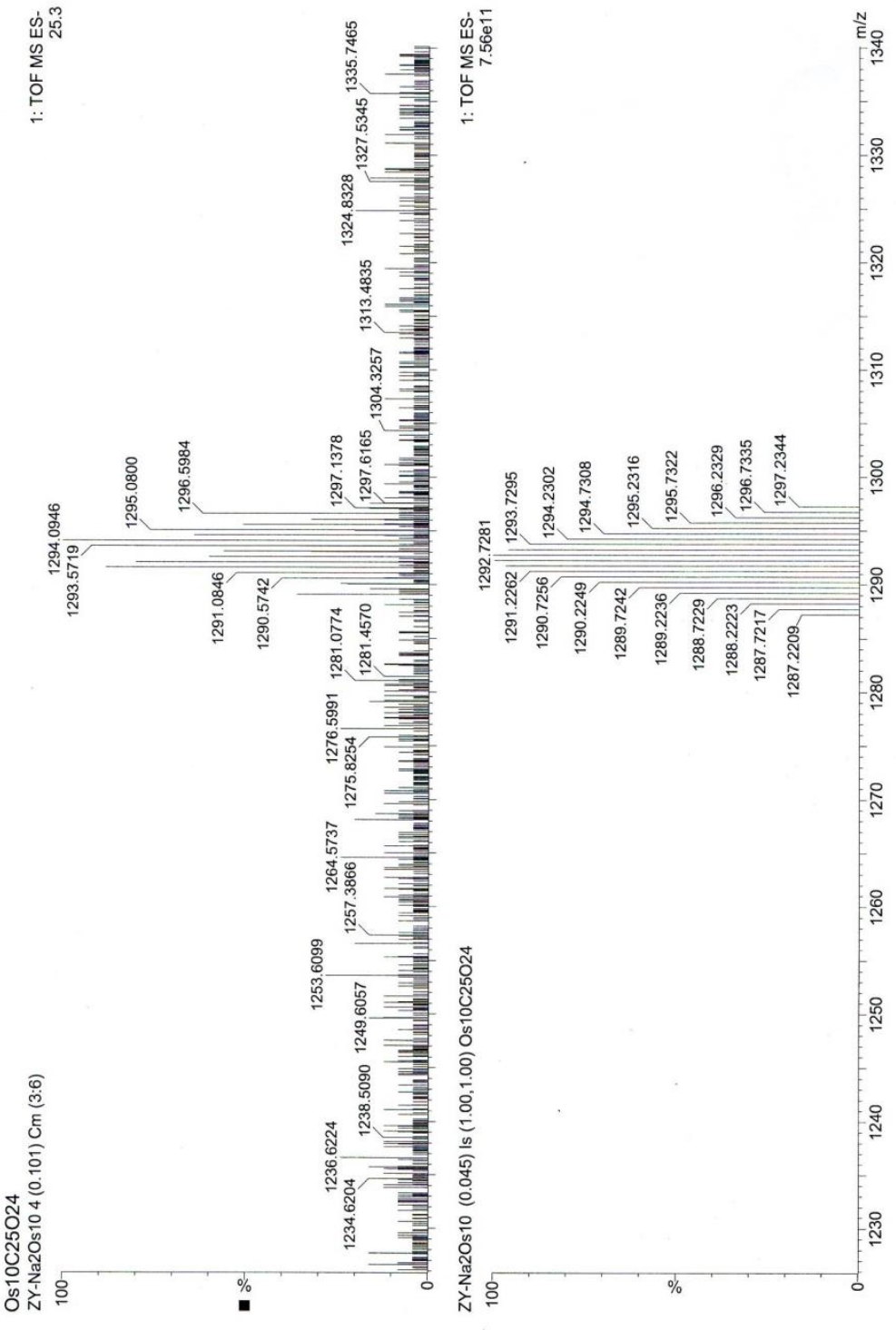

Figure S26. HRMS-ESI spectrum of cluster **9** (top). The calculated isotopic pattern is as shown at the bottom.

Table S1. ICP-MS analysis of Os in various organs of animals 24 h after injection of **9**.

a) Animal 1 (mass = 23.1 g)

Tissue	Tissue mass (dried) / mg	Elemental concentration of Os / ppb	Mass of Os / µg	Mass of Os per tissue mass / ng mg^{-1}
Liver	363.28	859.50	85.95	236.6
Spleen	44.20	105.81	10.58	239.4
Lungs	36.07	10.47	1.05	29.0
Tumor	11.82	5.70	0.57	48.2
Kidneys	114.53	4.82	0.48	4.2
Heart	33.09	1.32	0.32	9.7
Brain	91.27	2.16	0.22	2.4
Blood (50 µL)	N. A.	1.79	0.18	3.6*

*Represented as mass of Os per fluid volume / ng μL^{-1}

b) Animal 2 (mass = 22.3 g)

Tissue	Tissue mass (dried) / mg	Elemental concentration of Os / ppb	Mass of Os / µg	Mass of Os per tissue mass / ng mg^{-1}
Liver	387.20	932.75	93.28	240.9
Spleen	38.01	48.55	4.86	127.7
Lungs	41.43	7.01	0.70	16.9
Tumor	27.03	1.25	0.13	4.6
Kidneys	117.58	5.19	0.52	4.4
Heart	44.31	1.76	0.18	4.0
Brain	94.73	1.01	0.10	1.1
Blood (50 µL)	N. A.	1.14	0.11	2.3*

*Represented as mass of Os per fluid volume / ng μL^{-1}

c) Animal 3 (mass = 21.0 g)

Tissue	Tissue mass (dried) / mg	Elemental concentration of Os / ppb	Mass of Os / µg	Mass of Os per tissue mass / ng mg^{-1}
Liver	361.55	927.50	92.75	256.5
Spleen	30.86	35.42	3.54	114.8
Lungs	37.22	25.79	2.58	69.3
Tumor	17.55	0.90	0.09	5.1
Kidneys	91.76	4.18	0.42	4.6
Heart	44.35	2.32	0.23	5.2
Brain	87.63	0.41	0.04	0.5
Blood (50 µL)	N. A.	1.14	0.11	2.3*

*Represented as mass of Os per fluid volume / ng μL^{-1}

d) Mean values

Tissue	Mass of Os per tissue mass / ng mg^{-1}
	Mean (± SE of mean)
Liver	245 ± 6
Spleen	161 ± 40
Lungs	38 ± 16
Tumor	19 ± 14
Kidneys	4.4 ± 0.1
Heart	6.3 ± 3.0
Brain	1.3 ± 0.6
Blood*	2.7 ± 0.4*

*Represented as mass of Os per fluid volume / ng μL^{-1}

Table S2. ICP-MS analysis of Os in various organs of animals 96 h after injection of **9**.

a) Animal 1 (mass = 20.1 g)

Tissue	Tissue mass (dried) / mg	Elemental concentration of Os / ppb	Mass of Os / µg	Mass of Os per tissue mass / ng mg^{-1}
Liver	311.45	777.31	77.73	249.6
Spleen	29.94	126.17	12.62	421.4
Lungs	26.56	3.56	0.36	13.4
Tumor	9.44	0.37	0.04	3.9
Kidneys	94.69	1.79	0.18	1.9
Heart	25.73	0.51	0.05	2.0
Brain	91.07	0.13	0.01	0.1
Blood (50 µL)	N. A.	0.28	0.03	0.6

*Represented as mass of Os per fluid volume / ng μL^{-1}

b) Animal 2 (mass = 20.0 g)

Tissue	Tissue mass (dried) / mg	Elemental concentration of Os / ppb	Mass of Os / µg	Mass of Os per tissue mass / ng mg^{-1}
Liver	314.38	732.42	73.24	233.0
Spleen	28.74	55.96	5.60	194.7
Lungs	31.75	1.82	0.18	5.7
Tumor	24.82	0.51	0.05	2.1
Kidneys	99.23	6.51	0.65	6.6
Heart	22.41	0.42	0.04	1.9
Brain	83.46	0.16	0.02	0.2
Blood (50 µL)	N. A.	0.23	0.02	0.5

*Represented as mass of Os per fluid volume / ng μL^{-1}

c) Mean values

Tissue	Mass of Os per tissue mass / ng mg^{-1}
	Mean (± SE of mean)
Liver	241 ± 8
Spleen	308 ± 113
Lungs	10 ± 4
Tumor	3.0 ± 0.9
Kidneys	4 ± 2
Heart	1.93 ± 0.05
Brain	0.17 ± 0.02
Blood*	0.51 ± 0.05*

*Represented as mass of Os per fluid volume / ng μL^{-1}

Table S3. ICP-MS analysis of background Os content in various organs in control animals (without the introduction of **9**).

a) Animal 1 (mass = 21.8 g)

Tissue	Tissue mass (dried) / mg	Elemental concentration of Os / ppb	Mass of Os / μg	Mass of Os per tissue mass / ng mg^{-1}
Liver	341.14	0.84	0.08	0.25
Spleen	33.86	0.39	0.04	1.15
Lungs	30.33	0.23	0.02	0.76
Tumor	13.15	0.22	0.02	1.67
Kidneys	103.46	0.46	0.05	0.44
Heart	36.89	0.31	0.03	0.84
Brain	90.78	0.28	0.03	0.31
Blood (50 μL)	N. A.	0.29	0.03	0.58

*Represented as mass of Os per fluid volume / ng μL^{-1}

b) Animal 2 (mass = 21.0 g)

Tissue	Tissue mass (dried) / mg	Elemental concentration of Os / ppb	Mass of Os / μg	Mass of Os per tissue mass / ng mg^{-1}
Liver	309.90	0.17	0.02	0.05
Spleen	24.06	0.13	0.01	0.54
Lungs	27.97	0.11	0.01	0.39
Tumor	5.89	0.16	0.02	2.72
Kidneys	102.63	0.15	0.02	0.15
Heart	37.17	0.12	0.01	0.32
Brain	88.43	0.13	0.01	0.15
Blood (50 μL)	N. A.	0.14	0.01	0.28

*Represented as mass of Os per fluid volume / ng μL^{-1}

c) Mean values

Tissue	Mass of Os per tissue mass / ng mg^{-1}
	Mean (± SE of mean)
Liver	0.15 ± 0.1
Spleen	0.8 ± 0.3
Lungs	0.6 ± 0.2
Tumor	2.2 ± 0.5
Kidneys	0.3 ± 0.1
Heart	0.6 ± 0.3
Brain	0.23 ± 0.08
Blood*	0.4 ± 0.2*

*Represented as mass of Os per fluid volume / ng μL^{-1}

Table S4. Calculation of the retention of Os in various organ tissues 24 h after injection of **9**.

a) Calculation of mass of Os administered into each animal

Percentage mass of Os in **9** = 72.26%

No. of moles of **9** administered into the animal = 200 μL x 500 μM = 0.100 μmol

Mass of **9** administered into each animal = 0.100 μmol x 2632.53 g mol^{-1} = 263.25 μg

Mass of Os administered into each animal (M_T) = (72.26/100) x 263.25 = **<u>190.23 μg</u>**

b) Estimation of the amount of Os in blood based on projected total blood volume

The blood volume of mouse was estimated to be 79 (77-80) μL g^{-1}.[12, 13] Hence, this value was used for the calculation of blood volume:

Estimated blood volume of animal 1 (A1) = 79 μL g^{-1} x 23.1 g = 1825 μL

∴ Mass of Os in blood of A1 = (0.179 μg / 50 μL) x 1825 μL = **<u>6.53 μg</u>**

Estimated blood volume of animal 2 (A2) = 79 μL g^{-1} x 22.3 g = 1762 μL

∴ Mass of Os in blood of A2 = (0.114 μg / 50 μL) x 1762 μL = **<u>4.02 μg</u>**

Estimated blood volume of animal 3 (A3) = 79 μL g^{-1} x 21.0 g = 1659 μL

∴ Mass of Os in blood of A3 = (0.114 μg / 50 μL) x 1659 μL = **<u>3.78 μg</u>**

Tissue	**Mass of Os (M_O) / μg**			**Percentage retention of Os in the tissue (M_O/M_T x 100) / %**			
	A1	**A2**	**A3**	**A1**	**A2**	**A3**	**Mean (± SE of mean**
Liver	85.95	93.28	92.75	45.18	49.03	48.76	47.66 ± 1.24
Spleen	10.58	4.86	3.54	5.56	2.55	1.86	3.33 ± 1.14
Lungs	1.05	0.70	2.58	0.55	0.37	1.36	0.76 ± 0.30
Tumor	0.57	0.13	0.09	0.30	0.07	0.05	0.14 ± 0.08
Kidneys	0.48	0.52	0.42	0.25	0.27	0.22	0.25 ± 0.02
Heart	0.32	0.18	0.23	0.17	0.09	0.12	0.13 ± 0.02
Brain	0.22	0.10	0.04	0.11	0.05	0.02	0.06 ± 0.03
Blood^	6.53	4.02	3.78	3.43	2.11	1.99	2.51 ± 0.46

^Estimation based on total blood volume of animals

References

1. G. O. Nelson and C. E. Sumner, *Organometallics*, 1986, **5**, 1983-1990.
2. M. P. Cifuentes, M. G. Humphrey, J. R. Shapley and K. Lee, *Inorg. Synth.*, 2007, 287-293.
3. C. R. Eady, P. F. Jackson, B. F. G. Johnson, J. Lewis, M. C. Malatesta, M. McPartlin and W. J. H. Nelson, *J. Chem. Soc., Dalton Trans.*, 1980, 383-392.
4. M. P. Cifuentes, M. G. Humphrey, B. W. Skelton and A. H. White, *Organometallics*, 1995, **14**, 1536-1538.
5. P. J. Bailey, M. A. Beswick, B. F. G. Johnson, J. Lewis, M. McPartlin, P. R. Raithby and M. C. R. de Arellano, *J. Chem. Soc., Dalton Trans.*, 1996, 3515-3520.
6. M. I. Bruce, N. N. Zaitseva, B. W. Skelton and A. H. White, *J. Chem. Soc., Dalton Trans.*, 2002, 3879-3885.
7. K. D. Johnson and G. L. Powell, *J. Organomet. Chem.*, 2008, **693**, 1712-1715.
8. A. Buehler, E. Herzog, D. Razansky and V. Ntziachristos, *Opt. Lett.*, 2010, **35**, 2475-2477.
9. A. Rosenthal, D. Razansky and V. Ntziachristos, *IEEE Trans. Med. Imag.*, 2010, **29**, 1275-1285.
10. J. Schindelin, I. Arganda-Carreras, E. Frise, V. Kaynig, M. Longair, T. Pietzsch, S. Preibisch, C. Rueden, S. Saalfeld, B. Schmid, J.-Y. Tinevez, D. J. White, V. Hartenstein, K. Eliceiri, P. Tomancak and A. Cardona, *Nat. Methods*, 2012, **9**, 676-682.
11. N. C. Burton, M. Patel, S. Morscher, W. H. P. Driessen, J. Claussen, N. Beziere, T. Jetzfellner, A. Taruttis, D. Razansky, B. Bednar and V. Ntziachristos, *NeuroImage*, 2013, **65**, 522-528.
12. B. M. Mitruka and H. M. Rawnsley, *Clinical Biochemical and Hematological Reference Values in Normal Experimental Animals and Normal Humans*, Masson Publishing, New York, USA, 1981.
13. J. E. Harkness and J. E. Wagner, *The Biology and Medicine of Rabbits and Rodents*, Lea and Febiger, Philadelphia, USA, 1989.